# 1 Response to reviewer 1

**The manuscript presents the application of the newly developed PCMCI algorithm for the detection of causal links in geophysical data, focusing on biosphere/atmosphere interactions. Applications of the algorithm is done using flux tower eddy covariance data, for fine temporal scale analysis, and satellite derived NDVI along with climate data are used for global scale analysis at coarser scales. The topic is important and clearly within the scope of Biogeosciences. Identifying and quantifying causation in geophysical data is crucial for understanding the interplay of the processes involved and developing models. The present manuscript is intended to my understanding to be primarily a proof of concept of the applicability of the PCMCI algorithm. While the paper is well written several parts need to be better clarified.**

We thank the reviewer for the support of the manuscript and further suggestions and address the points below.

**Specific comments:**

- **I find the description of the algorithm on the paper slightly confusing (in particular for a Biogeosciences audience). I believe that the reader must refer to (Runge et al.,2018) to understand the basic principles behind the algorithm. I strongly suggest the authors to restructure and clarify this section. Simplifying the description and reporting the algorithm details as supplementary information could benefit the fluency of the manuscript.**

  We improved the accessibility of the method by restructuring of the existing text and adding an introductory subsection to the method section. Here we explained how PCMCI relates to existing methods and what its key concept is. This helps the reader to gain a more intuitive understanding of aim and concept of PCMCI. More detailed description of assumptions, independence tests and the two parts building PCMCI are then given in the following subsections.

  Please refer to the sections 2.1, 2.2, 2.3 and 2.4 in the marked up manuscript for details.

- **The synthetic test developed to quantify the skill of the algorithm, when its assumptions are not valid (e.g. seasonality, heteroscedacity) is clearly important. However, it is not currently clear how the results derived from this analysis can be generalized beyond the Hainich site. Emphasis should be given on the transferability of the magnitude of expected biases at a global scale.**

  We believe this may be a misunderstanding. The synthetic test did not focus solely on the Hainich site. The impression might be given, as a few plots (time series and networks) are showing as an example the results from Hainich. We used radiation data from 72 FLUXNET sites to run the model. Therefore, the results are not bound to the conditions at Hainich.

  To clarify this we changed within the first paragraph of section '2.3.1 Artificial Dataset - Test Model' the sentence:

> Using time series of measured global radiation (Rg) we created three artificial time series that conceptually represent temperature (T), gross primary production (GPP) and ecosystem respiration (Reco)."

To:

> The artificial dataset was created using a test model which takes time series of measured global radiation (Rg) and creates three artificial time series that conceptually represent air temperature (T ), gross primary production (GPP) and ecosystem respiration (Reco).[....]

With further explanations in line 19ff on page 9:

> The model was fitted to real observational data (using radiation, temperature and land-atmosphere fluxes) of daily time resolution, measured by eddy-covariance method (Baldocchi et al., 1988; Baldocchi, 2003) from FLUXNET, by minimizing the sum of squared residuals using the gradient descent implemented in the Optim.jl package (Mogensen and Riseth, 2018). We fitted the model to 72 sites listed in Table B1 given in the Supplementary Material section.

We think that this adjustment should clarify that we are not focusing on the Hainich site only.

- **In a broader sense, a key question is why would the authors use a procedure for the identification of causal links, when the basic assumptions of the procedure are violated by the data?**

  Every statistical method comes with a set of assumptions which are required to assure interpretability of the results. In our case the assumptions guarantee theoretically that the method will estimate the true causal graph. In a real world study case, those assumptions are typically not fully met. This can be already the case for linear regression (e.g., perfect normality). Our work addresses exactly the point of how well PCMCI works under violations of the assumptions, that is, how robust the method is regarding realistic violations occurring in practice. PCMCI in conjunction with ParCorr possesses several attributes which favour its use, as shown in our analysis: high detection power, interpretability, and computational efficiency. We aimed to identify whether PCMCI and ParCorr could in fact deliver reliable results using artificial and real data.

- **I believe the authors should better explain why the proposed algorithm in more efficient than e.g. the spectral Granger causality algorithm proposed earlier by Detto et al.(2012), which, to my understanding, is inherently non-parametric and not sensitive to periodicities.**

  Thanks for pointing out the need for a more detailed comparison to other methods. This is basically in line with Reviewer 3 who, however, suggested the comparison to another approach. We totally agree on the importance of such comparisons but regard numerical analyses evaluating other methods to be out of scope of this paper. Nevertheless, we agree that we could better describe the specific characteristics and benefits of PCMCI in conjunction with the independence test ParCorr.

PCMCI is computationally efficient, has proper significance testing and attribution of link strengths. As we observe, the seasonality is an obstacle for PCMCI and might be better handled with a spectral method. But, to the best of our knowledge, spectral Granger causality is also bound to causal stationarity. Thus, within an analysis spanning (possibly) several years and seasons, one would assume a constant network structure throughout time (same network structure in winter as in summer). However, this is not the case, as we could show in our analysis of the Majadas ecosystem.

- **In Fig2 it is shown that with an increasing sample size, the fraction of falsely identified causal links increases, when the algorithm's assumptions are not valid. This can be a significant drawback as the best datasets (i.e. with long records), are more prone to errors. The authors should better discuss this.**

  To analyse long record time series data one has to question whether causal stationarity is fulfilled. As we have seen in the example of the Majadas dataset, strong differences in the dependence structure occur for different months of the year. Accounting for causal stationarity still does not conflict with analysing long data records with PCMCI, because by applying a proper mask one can estimate the network structure for one month or season within multi year time series (which is similar to our mask used in the Majadas dataset: taking only noon values but for consecutive days). Such a mask increases stationarity and therefore reduces an inflated false positive rate.

  This is partially discussed already on page 20 line 3 to 20. To further clarify we will modify the submitted paper as follows:

  We replace line 13 and 15:

  > Much of the influence of heteroscedasticity is also removed when limiting the analysis to a specific time period, i.e.season, which makes the data causally stationarity (cf. Sect. 2.1). For example, the link from radiation to GPP vanishes in winter as there is mostly no active plant material left.

  With:

  > The increasing FPR with increasing time series length can further raise doubts regarding the analysis of long time series. For such an analysis, though, the assumption of causal stationarity should first be assessed. For example, the link from radiation to GPP vanishes in winter as there is mostly no active plant material left. To account for causal stationarity, the analysis should be limited to time series sections where the causal structure is expected to be similar. This is typically done by limiting the analysis to a specific time period (i.e. 'masking'), e.g. a

specific season, month, or time of the day. Such masking reduces additionally further influences of remaining seasonality or heteroscedasticity.

- **If I understood correctly, it is shown that for the baseline case, the algorithm cannot robustly identify the true causal non-linear links (as expected). However, the identification rate increases incorporating seasonality (which I presume also violates the stationarity assumption of the algorithm), which is counter intuitive. The authors in their discussion attribute this behaviour to the variance of the parent variable. Can the authors discuss how this artefact can limit the range of applicability of the procedure for global scale applications (i.e. differences in regions with distinct seasonality or not)?**

  Seasonality constitutes a common driver in this model. In general, such common drivers increase the dependence among the variables and, hence, lead to a higher detection rate for true links (TPR) as well as a higher false positive rate (FPR) for absent links since this driver is not conditioned out properly. Therefore it is not counter intuitive that both the TPR and the FPR rate increase in the seasonality model. To reduce the effect of seasonality further, we suggest to use a mask or use deseasonalized time series.

  We added following sentences to section 4.1.

  > Seasonality and heteroscedasticity constitute violations of the stationarity assumption underlying the independence test ParCorr. Seasonality constitutes a common driver in this model. In general, such common drivers increase the dependence among the variables. and, hence, lead to a higher detection rate for true links (TPR) as well as a higher false positive rate (FPR) for absent links if this driver is not conditioned out properly. This additionally causes the TPR and the FPR rate to increase in the seasonality model. As shown in [**?**], including the cause of the non-stationarity as an exogenous driver in the analysis allows PCMCI to regress out its influence on the other variables. However, for ParCorr this is only valid if the dependence on the non-stationary driver is linear. Therefore, the regression on $\mathcal{R}g$ fails for $\mathcal{GPP}$ and $\mathcal{R}eco$ in the test model. With this ill-posed setting, the probability to detect false links increases with increasing time series length or when more periods are included.

# 1 Response to reviewer 2

**The presented manuscript presents an interesting and novel approach to better understand biosphere-atmosphere interactions. The paper is clearly of interest for the scientific community and fits well in the scope of the Biogeosciences journal. While moving on from the classical correlation approach is needed and of great interest, because causality is modern topic and no so broadly used, the paper needs to do a better effort to introduce the topic in an easy way to the community in order to be published. Actually, it is difficult for me to review the results of the paper until the methods are more clearly exposed to the reader.These are my specific comments:**

We thank the reviewer for the support of the topic. The accessibility of the method has been criticised also by reviewer 1. In a revised version of the manuscript we will aim for an improved accessibility of the method. Please refer to your specific comment for further details.

Introduction: **I miss a paragraph showing the limitations of the classical correlations analysis, when the failed, when causality approaches did better and why...**

We see the benefits the reviewer aims for by requesting such a paragraph. We do not claim correlation analysis to be wrong, if applied correctly. The issues arise, if one moves beyond certain boundaries within the interpretation of the results. A correlative analysis does not fulfill requirements for a causal interpretation. Any method which brings us closer to causal interpretability of a dependence structure increases the information content of the analysis. This is our motivation to test a causal inference method that is more sophisticated than the mere use of correlations.

This argument is further motivated, first by citing literature which showed an improved interpretability using causal methods rather than correlation (cf. Detto 2008, but also Runge2019 and others), and second by highlighting the differences of the estimated dependence structure using lagged correlation and PCMCI (cf. Fig. 1 or Fig. 4 and F1).

Methods: **In general, as I said, the methods are hard to follow. I suggest to simplify/restructure the section to facilitate its understanding. The section 2.1.2 is probably the most confusing to me, I recommend to include a flowchart to visualise the algorithm.**

We improved the accessibility of the method by restructuring of the existing text and adding an introductory subsection to the method section. Here we explained how PCMCI relates to existing methods and what its key concept is. This helps the reader to gain a more intuitive understanding of aim and concept of PCMCI. Detailed description of assumptions, independence tests and the two parts building PCMCI are then given in the following subsections. Further, we added a schematic now available as Figure A1.

Results: **Line 5, page 12, replace "stonger" by stronger.**

Thanks for noticing and pointing out this spelling mistake.

Discussion: **Lines 7-11: After reading the paper, I am still not convinced that using a linear in-dependence test is the way to proceed. I think you have to demonstrate it with an example. Perhaps, you can run your artificial dataset tests using a non linear rank independence test (spearman's correlation) and compare the results. These results could be added to an appendix to better support your statements if that's the case.**

We added analyses using Gaussian-process regression and distance correlations to the supplementary section. Spearman's correlation is not applicable as it is not an conditional independence test.

Within the introduction of the discussion, we refer to these results. Specifically, on page 19 line 11 we add:

> To further convince the reader we performed analyses on the observational datasets using Gaussian regression and distance correlation as an independence test. These results show similar patterns but due to the low sample sizes exhibit worse statistical significances.

For example, Fig. 1 is comparable to Fig. 5 from the manuscript. The difference is that 1 is calculated using Gaussian-process regressions and distance correlations as independence test (GPDC). The two figures show a similar seasonal behaviour and even good agreement in detected links. Note that GPDC only yields positive link strengths. Further, the strength values estimated with GPDC are rather weak due to the low number of datapoints and the larger sensitivity of that method to the sample size.

An other example is given in Fig. 2. Here the figure is not one-to-one comparable with Fig. 6 of the manuscript because significances of an analysis using GPDC have been too (due to too low sample sizes) low to perform the same analysis. Instead we plotted the link strengths of radiation, temperature and precipitation on NDVI at lag 0 and 1. At lag 0, GPDC detects some influence of temperature (and radiation) in boreal regions. At lag 1 precipitation influences mostly arid regions.

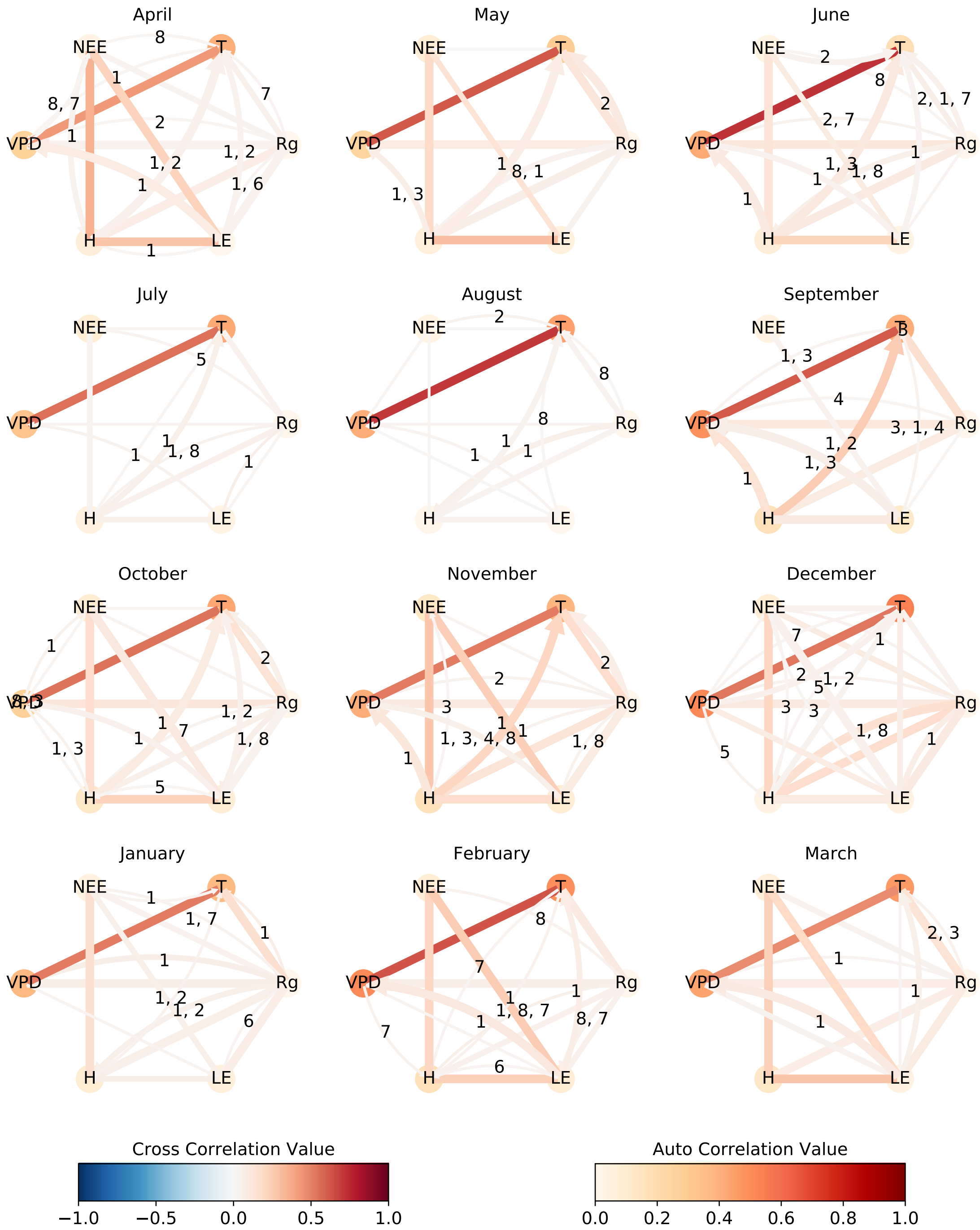


Figure 1: Same as Fig. 5 of the manuscript but the analysis was performed using a non-linear independence test. The number of significant occurrences of a link is given by its width. The link strength, given by the link color, is calculated by averaging the significant links of the towers. The link's lag is shown in the centre of each arrow, sorted in descending order of link strength. The resulting graphs are shown for April 2014 till March 2015. The significance threshold is 0.01

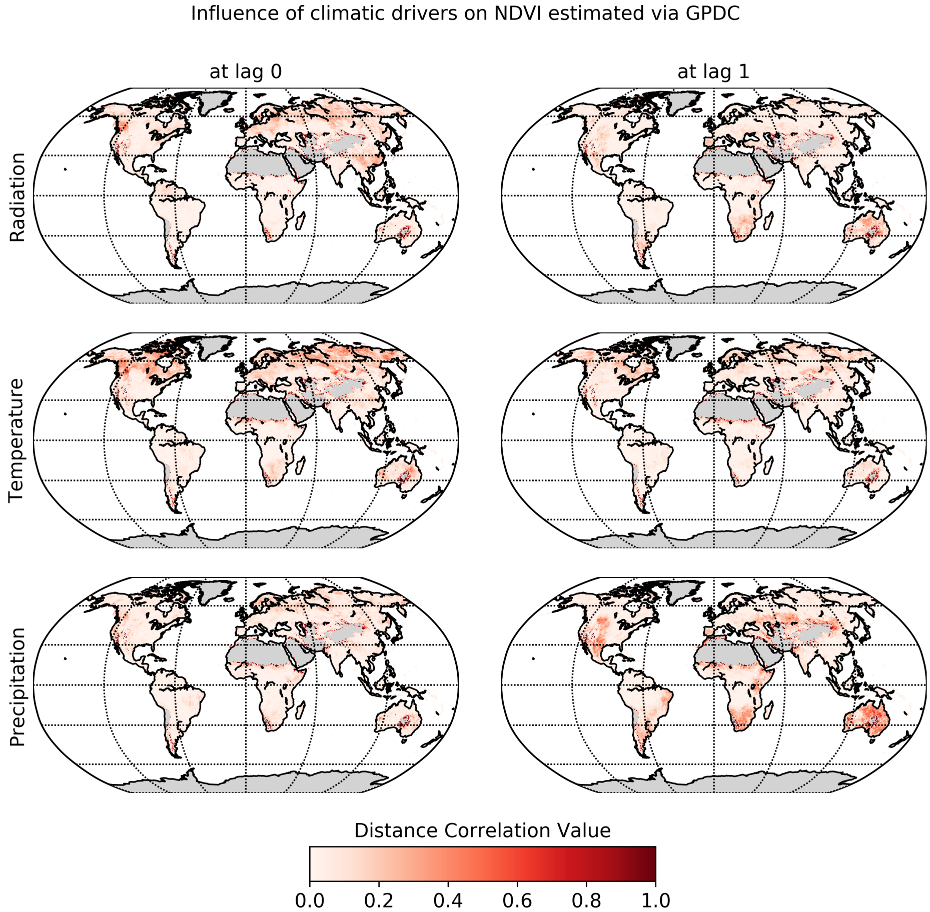


Figure 2: Influence of climatic drivers on NDVI as calculated by PCMCI in conjunction with the non linear independence test GPDC. The first and second columns show the estimated causal influences of climatic drivers on NDVI at lag 0 and 1, respectively.

# 1 Review 3

**This is Ben Ruddell writing; I waive anonymity for this review. When I saw this paper come across my desk it caught my attention, because I have been working on similar topics and also following the authors' work for several years. In general, I like this paper and after reading it I would like to see it published in this journal, with some changes. This general area of work needs a lot more attention because of the promise of the general approach and the urgency of getting our inference and modeling right for this kind of complex and coupled system. Thank you for this effort! After working on this kind of paper for more than a decade (and contemplating many reviews of my own work) I've come to the opinion that we need to move past a focus on innovating methods and toward the challenge of showing how the methods can be used to produce actionable and fundamentally novel insights- or to test process theories in science. If we cannot use advanced inference techniques to learn about these systems or critique previously inaccessible scientific ideas, these methods will continue to fall on deaf ears, so to speak. So, I challenge the authors and anyone else listening to move forward aggressively with the intent to apply causal networks (Process Networks) and advanced inference techniques to interrogate scientific hypothesis and learn about systems. The current paper could do more along these lines, with added investment, by(for instance) comparing its statistical results with expectations from climate or ecological models, etc.**

Dear Dr. Ruddell, thank you very much for your support and helpful advice. We fully agree that it is not enough to test and advocate for a new method only. However, in order to 'learn about these systems or critique previously inaccessible scientific ideas' the method of use has to be understood in its behaviour first. As PCMCI has not been tested or applied within the context of biosphere–atmosphere interactions to date, this was a necessary step to take before addressing specific scientific questions. The latter will be the aim of following studies, which will build upon the identified strengths of PCMCI. Further, testing or comparing the network structure between models requires non deterministic dependencies which, however, is typically not given.

In the following we try to respond accurately to your questions and comments and will try to integrate those as far as possible.

**Before beginning the review, based purely on the expectations raised by the very broad title of the paper, I already had a few questions about the paper. I will pose and then evaluate those questions before moving on to line by line comments.**

1. **Is the now-substantial body of literature on this topic adequately summarized and cited, giving credit where credit is due? Papagiannopoulou et al is cited twice, but the similar paper Seddon et al. 2016 is not cited; please cite appropriately. Please review GeoInfoTheory.org, which has a nice list of publications on related topics (https://geoinfotheory.org/reference-list/). In**

**particular,there are a few recent papers that should really be cited appropriately in your paper,because they are recent and narrowly within the scope of your literature review; these treat global land-atmosphere interactions and feedbacks using similar methods to your own. Please describe in your introduction, methods, and/or results as relevant, how does your work relate to these? Yu et al. 2019 in GCB is especially important. A list of references that would seem to be highly relevant follows.** [please refer to original comment to see reference list]

Thank you for this supportive comment. We improved the discussion of related literature. There we restructured paragraph 3 and 4 of the introduction which are now spanning from page 3 line 17 to page 4 line 13.

2. **Is the concept and any methods used for "causality" adequately posed and defended? You can expect such a strong claim and wording as "causal graph" to be aggressively challenged by readers and reviewers in this paper and any others using the term, fora long time to come. Renaming "correlation" or "information flow" to "causation" is a major and very aggressive departure from our disciplines' wording and conceptualization during the long and mature history of statistical inference, and requires very strong justification. Granger causality has never really been "causality"; it's a type of conditional time-lagged cross correlation. Please understand my point here; I'm not asking for you to give up on the use of "causal" language, but I am strongly requesting that you spend at least a paragraph in the introduction or methods section of this paper (and others, for the foreseeable future) to argue and explain to the reader exactly what is,and is not, meant by "causal" in this context. It is otherwise too strong a term to be using. As a more general comment, it's extremely important for us to reach a consensus about what to call things. This is an iterative community process of communication that works through conversation and engagement, and through clarification about what is the same and what is different. It's not my place to decide whether we should be calling something a "causal network" or a "Process Network", but I do insist that we have the conversation. For the purposes of this paper, this means citing my recent & prior work,and that of others, and trying to explain exactly how your terms relate to our terms for similar things, and proposing what you understand the similarities and differences to be; this is particularly important when writing a methods paper such as this one under review here.**

   Indeed the prefix "Granger" is always used in Granger causality analysis to differentiate it from some stronger form of causality. The same applies to concepts of Information Flow or Transfer Entropy, which avoid the term causal. This stronger form has so far remained elusive, but it is the merit of seminal works by Judea Pearl (Pearl 2009) and others to put the term causal on a solid mathematical basis. This is the framework of causal graphical models (Spirtes 2000, Pearl 2009) which lays out the assumptions under which graphs (aka networks) estimated based on conditional independencies can be interpreted causally. Not least through his popular science book (Pearl 2018), Pearl has advocated to overcome, as he states, the 'mental barrier' of using causal language— as long as it is used together with the assumptions required. And these assumptions have to be thoroughly discussed in any analysis. This is exactly the goal of our work. PCMCI belongs to the causal graphical model framework and under the assumptions listed in the paper (refer to Sect) and in the limit of infinite time series length PCMCI converges to the true causal graph, which is why we use the term causal. As we deal with finite sample length and partially unfulfilled assumptions we mention several times, that spurious links can appear (in excess to the expected FPR) and that each detected link has to be interpreted carefully.

This is now mentioned at the end of the new Paragraph 'Evolution of PCMCI from information theory' of the method section.

3. **Is there anything new here, and is that made clear? Yes! PCMCI is put through some rigorous tests for both satellite and 30m flux data and appears to hold up well; this is novel and interesting as a methodological development. However, in my opinion, it is important when describing this method in the methods section that you distinguish it precisely and detail from other similar methods,explaining its relative advantages and disadvantages. There are lots of other methods out there that have used Granger-adjacent directed coupling statistics in various application contexts. In this precise context, my 2009 papers you cited (and several since)used 30 minute flux tower time series data to determine atmo-bio networks, identifying ranges of statistically significant time lagged couplings, and also studies periodicity and noise in the method, calling these resulting patterns "Process Networks", and distinguishing the most "causally" relevant couplings using a Tz metric that compares directed vs correlative information flows. This is a well worn topic in 2019, so it's not sufficient in a methods paper to contrast your method with correlations anymore. Contrast your method precisely against others that claim similar goals and results, please. Why should we use PCMCI instead of one of several other existing similar methods?How would the results differ in theory and in practice? Should we use PCMCI in this case, and use Ruddell et al. 2009a "Tz" in another case? What are the pros and cons? Because this paper focuses on methods, it needs to be much more specific about how these methods relate to other adjacent methods and conflicting/overlapping terminologies already in use; this engagement is how we will build our community's knowledge and practice. (your treatment of the underlying assumptions is a strength of the paper and should help make these distinctions clear; thank you for this attention to detail here.)**

   Thank you for the above comments. We improved the accessibility of the method by restructuring of the existing text and adding an introductory subsection to the method section. Here we explained how PCMCI relates to existing methods and what its key concept is. This helps the reader to gain a more intuitive understanding of aim and concept of PCMCI. Detailed description of assumptions, independence tests and the two parts building PCMCI are then given in the following subsections.

However, an in-depth numerical comparison of the available methods is beyond the scope of the manuscript, and partially already done in Runge et al. 2018 and 2019. There are several causal inference methods available, with multiple additional modifications. Picking only one or two of them (e.g., Tz statistic of Ruddell et al. 2009) would unavoidably be rather arbitrary. We agree that this comparison is important but might be best tackled in a separate study, maybe even in a combined effort. Such a comparison study would help users choose the most suitable method for each specific application, rather than addressing any specific question with the method at hand, as it is common practice. See also the causality benchmark platform www.causeme.net which addresses method comparison on a growing number of benchmark datasets.

4. **Is the very broad title justified, or is the paper actually about something much more narrow and specific?By the end of the abstract, I decided "negative" on 4. because this paper appears to be not a review or synthesis of the broad topic of causal networks in the bio-atmo-geo-sphere as implied by the title, but instead a methods case study establishing the robustness of a proposed method MCMCI in two land-atmosphere contexts. I suggest a much narrower title, like "PCMCI robustly identifies biosphere-atmosphere interdependencies", or some such. It is very important to use an accurate title that is not over-broad. The title directly summarizes the question and/or findings, in a nutshell.An overbroad or inaccurate title is grounds for rejection in my view.**

   Thank you for this advice. We renamed the title to "Estimation of causal networks in biosphere-atmosphere interaction: The PCMCI approach".

**Line by Line Comments**

Sec. 2.1 **I've followed the derivations in Runge et al. (various, 2014-2018) and I don't have a problem with the methods. However, I have not seen here or in Runge et al. (various) an explicit comparison of the MCI approach with Ruddell and Kumar's(2009a) "Tz" or zero-lag ratio method for the disambiguation of "strongly causal" versus "common-source causal" indicated couplings. There appears to be a lot of shared intent and intuition here, and possibly some very similar (but differently named) mathematics and assumptions. Please explain what is similar or different.**

PCMCI and Tz are two quite different approaches: PCMCI is a multivariate causal network estimation approach, Tz is bivariate and, at least in general, cannot exclude common causes or indirect links. Tz is a bivariate Transfer Entropy (TE) divided by the zero-lag mutual information

(MI). Ruddell and Kumar's(2009a) give a "coupling type" classification regarding the coupling interpretation of different values of TE and MI. However, any bivariate analysis is difficult to interpret causally since common drivers can both increase or decrease a MI or TE. For example, a significant MI and TE with TE ¿ MI, classified as "forcing dominated coupling" in Ruddell and Kumar's(2009a), can be the result of a common driver that drives X and Y in different ways. Hence, PCMCI and Tz are difficult to compare directly.

Pg.20-10 **This discussion on "causal stationarity" and limitation of study to one season or system state appears to be treated in Ruddell and Kumar 2009(b) (second half of the paper you cited) under the terms "local" and "global" stationarity. What's the relationship here, please?**

We studied the paper "Ecohydrologic process networks: 2. Analysis and characterization" by Ruddell and Kumar. We could not identify a definition of local or global stationarity. To our understanding the terms 'local' and 'global' are used in the context of choosing the bounds for the binning intervals in the estimation of the conditional probability densities. A local scheme refers to a binning interval chosen by the minimum and maximum values of the month. A global scheme refers to the binning interval that is chosen by the minimum and maximum values of the whole time series or dataset. The global scheme is chosen if a comparison between process networks is intended.

Causal stationarity means: A process $\mathcal{X}$ with graph $\mathcal{G}$ is called causally stationary over a time index $\mathcal{T}$, iff for all links $X^i_{t-\tau} \to X^j$ in the graph $X^i_{t-\tau} \not\perp\!\!\!\perp X^j \mid \mathbf{X}^-_t \setminus \{X^i_{t-\tau}\}$ holds for all $t \in \mathcal{T}$. An example: The influence from radiation to temperature exists in both summer and winter, it might weaken or strengthen but as the physical mechanisms remain active, the link satisfies causal stationarity through out the year. In contrast, the influence of radiation on photosynthesis in a deciduous forest exist in summer but can not exist in winter if no photoactive plant material is present. Thus causal stationarity is violated if the whole year is included in the analysis. Limiting the analysis to specific periods in time, e.g. summer, leads to causal stationarity. This masking in time in PCMCI could be done manually/fixed time intervals, e.g. monthly, or by choosing the mask for a specific value range of one specific variable, i.e. GPP or Rg. The latter might remind of the above mentioned local and global binning but still only marginally, from our perspective.

We noticed that this explanation is missing in the method section. We added it accordingly.

Pg.21-20 **Although it isn't the focus of your paper, Kumar and Ruddell (2010, Entropy) and some of my more recent papers (Yu et al., Gerken et al.) have shown very strong changes in coupling strength across space, as well as across time. I wouldn't make the claim that "the interaction between biosphere and atmosphere is expected to change only marginally across space" in the absence of strong arguments supporting this. I've argued the opposite in several recent papers- I've argued that the Process**

**Network characterizing these systems and their states changes dramatically between places and times, and that this represents a qualitative shift in how the systems are functioning. (note that I'm not arguing that physics changes, only that its structure and expression in a complex system changes dramatically)...please engage with this argument,or remove the claim.**

The claim "the interaction between biosphere and atmosphere is expected to change only marginally across space" was used only in the context of the Majadas ecosystem and within this context we regard it justified and well supported: This ecosystem is a rather homogeneous Savanna. Within this ecosystem three eddy-covariance towers are situated within a distance of up to one kilometre (app.). At such spatial scale, climatic conditions are very similar. Due to the homogeneity of the ecosystem "interaction between biosphere and atmosphere is expected to change only marginally across space".

We clarified that this statement by adding 'across space within this ecosystem' to the sentence 'Thus, also the interaction between biosphere and atmosphere is expected to change only marginally across space within this ecosystem'.

We again emphasize that PCMCI and the Tz measure used in the referees studies cannot be directly compared and any discussion on "strong" or "weak" couplings has to take into account whether the measure is multivariate or bivariate, since excluding the effect of common drivers can strongly change the value of a measure.

Pg.21-25 **Most of my papers have focused their analysis and presentation of results on a single "most significant" time lag (usually chosen as the first/shortest peak lag in mypapers, called the "characteristic time lag" in my papers), or an average across a range of time lags (usually subdaily ¡18hrs) because of the extreme challenge of interpretation posed by a large number of statistically significant coupling links. Separating out every conditionally "momentary" coupling is not hard to do mechanically, but interpretation and communication is devilish. I think you're running into this problem here. Once we move past conditioning couplings on zero-lag correlations, it's not clear where to stop or how to interpret the results. I'd hope that PCMCI could add some clarity, but I'm not convinced based on this discussion that it is helping. Please comment and clarify if possible, or at least explain how what you're doing is different here from what Ruddelland Kumar 2009 did with T, I, Tz, canonical coupling types, and characteristic timelags. If possible, also engage with Goodwell and Kumar (recent) who have attempted to split out redundant, synergistic, and independent couplings in the land-atmosphere coupling context.**

We agree that interpreting a process network incorporating many lags for one dependence can pose difficulties. That is why we omitted a detailed analysis/study of the monthly Majadas networks. Yet, we also did not want to aggregate or focus on one lag as this would have reduced the information content of the analysis. An averaging of lagged links, for example, would have caused a strong deviation in link strength for the dependence H→VPD in Fig. 4 (August) among the towers. $I(T \rightarrow VPD)_{LMa}$ would be nearly 0 while $I(T \rightarrow VPD)_{LM1}$ and $I(T \rightarrow VPD)_{LM2}$ would be around 0.25. This is due to the possibility of negative coupling strengths using ParCorr. The dependence H→VPD appears at lag 1 and 3. The confidence intervals of the strength values from the three towers are overlapping for both lags, but as the link H→VPD at lag 3 is rather weak, only one crosses the significance threshold.

Defining the maximum lag might be indeed difficult from a physiological/physical perspective. In Runge2018a following is suggested: "Choice of $\tau_{max}$: The maximum time delay depends on the application and should be chosen according to the maximum physical time lag expected in the complex system. In practice we recommend a rather large choice that includes peaks in the lagged cross-correlation function (or a more general measure corresponding to the chosen independence test), because a too large choice of $\tau_{max}$ merely leads to longer runtimes of PCMCI, but not to an increased estimation dimension as for FullCI."

Due to the differences between PCMCI and the Tz statistic laid out above, we omit further comparison.

Pg.22-15 **I am not convinced by biweekly or monthly scale correlation analysis in satellite or climate data represents causation in any real or approximate sense. There are several problems here. First, these data are modeled and abstracted several levels beyond primary observations, so patterns cannot be relied upon to strongly represent causal realities as well as in-situ flux data. Second, once we move past subdaily timelags, we are well into the scales dominated by diurnal cycles, synoptic weather cy-cles and by seasonal rhythms, so it is hard to distinguish signal from noise when the"noise" is an overwhelmingly energetic diurnal, seasonal, or synoptic cycle. Third, we already have strong reason to believe that the main process timescales are subdaily, due to e.g. our flux tower analyses, so we must presume that super daily or monthly timescales indicated by the methods are merely echoes and confounding correlates of shorter timescale processes unless we can prove otherwise (e.g. through robust conditioning against shorter lags)- and that proof is not possible using coarse time resolution data. This is a basic problem with attempts to use satellite and coarse time resolution gridded data to establish "causal" relationships, and I haven't seen it adequately addressed in this paper or prior papers attempting similar. What am I missing here, please? Please explain how your method addresses these three problems. This gridded/monthly analysis may be a "bridge too far", so to speak, for this paper; it's different from and a weaker argument than your eddy covariance analysis, with several layers of practical problems weakening the conclusions.**

This comment might be addressed by addressing comment 2. Causal relationships are best examined by perturbing the system at a specific time and state (variable) (do calculus of Pearl). Though such experiments are usually not feasible in a controlled manner within Earth system sciences. Therefore, we (as a community) rely on the estimation of causal dependencies from time series and can only detect the signal imprinted in the time series. The signal of interactions depends on properties of the interaction itself, i.e. the strength,type and pattern, but also the signal-to-noise ratio, i.e. measurement noise, time sampling intervals and time aggregation. Therefore, the signal of interactions detectable within the time series (i.e. dependence within the conditional probability distributions, which using Markov condition determines connectedness in graph) might not correspond to the actual physical interactions anymore, but might very well allow valuable insight. Especially when trying to evaluate and compare dependence structures within model time series. Further, under aggregation information from fast interactions will be lost (and maybe visible as contemporaneous interactions in our networks) but processes which are dominant on larger time scales might appear as their signal is improved due to aggregation.

Further, Ruddell and Kumar 2009 and Krich 2019 find links on timescales below 30 min on 30 min time resolution fluxdata. Having the above in mind, i.e. keeping in mind that the time sampling interval determines the appearance of the causal graph, one can not even speak of the 'true causal relationships' using 30min resolution data. If links appear that happen on faster time scales than the time resolution, they will be shown as contemporaneous links (undirected) in our networks. In the method section, we state, that spurious links, both contemporaneous and lagged, can appear. This will be further elaborated in a revised manuscript.

Fig. 6,7 **These results are begging for a detailed comparison with Yu and Ruddell etal., published earlier this year in Global Change Biology, which attempts a very similar analysis but uses an extrapolation of 30m flux data derived couplings to the global terrasphere rather than monthly gridded data. Please provide this comparison.**

With all respect, we do not fully agree on the level of similarity between these two studies. Without a doubt the performed study "Anticipating global terrestrial ecosystem state change using FLUXNET" by Yu and Ruddell et al. 2019 is very interesting and we actually had similar ideas for another study. To explain why we prefer to omit a comparison with this study, we briefly summarize the method and subsequently give the reasoning.

Yu and Ruddell (2019) calculated two bivariate transfer entropy couplings (Temp-NEE, Precip-NEE) on monthly time periods of the available time series data of 204 Fluxnet towers. Thus they obtain a network per month which can be translated to monthly time series of couplings. These couplings are fitted with a specific model (using monthly averages or sums of Rg, Temp, Precip, EVI) to estimate an elasticity of that coupling to each 'driver'. Those elasticities are upscaled to global scale using an artificial neural network. Those maps of upscaled elasticities shall be compared to

PCMCI strength values.

The choice of variables for the coupling calculations are based upon: (quote from the paper) "an eddy covariance tower's process network can be approximated using three functional subsystems: Synoptic, Atmospheric boundary layer (ABL), and Turbulent. We choose an essential timeseries from each of those three subsystems: for the Synoptic subsystem, air temperature; for the ABL subsystem, precipitation; and for the Turbulent subsystem, net ecosystem exchange of carbon".

We believe a comparison is not straightforward because of two reasons: The quantity we plot in Fig. 6 and 7 is a conditional independence measure, i.e. partial correlation coefficient between time series residuals at monthly resolution in a multivariate analysis. The plotted elasticities in Fig. 3 of Yu and Ruddell et al. 2019 represent an upscale of a specific co variation (an exponential model) of a conditional independence measure, i.e. bivariate transfer entropy between time series at 30 min resolution, to monthly aggregates of climate and phenology variables. We have difficulties to relate these two quantities with each other. Furthermore, We want to validate the outcome of PCMCI. Thus we preferably compare our results to studies which calculate a dependence measure on approximately the same data as we used.

Second, Fig. 6 and 7 of our study show the dependence of phenology (NDVI) on climatic drivers. Fig. 3 of Yu and Ruddell et al. 2019 shows the elasticities of NEE to both climatic and phenological drivers. Fluctuations and responses of NEE and NDVI to climatic factors happen on very different time scales. Further, NEE and NDVI are difficult to compare in the first place.

We hope that we could convince you that the comparison of our global case study to Wu et al. (2015) and Papagiannopoulou et al. (2017b) is better suited for verification purposes than a comparison to Yu and Ruddell et al. 2019.

# ~~Causal networks~~ Estimation of ~~biosphere–atmosphere interactions~~causal networks in biosphere-atmosphere interaction: The PCMCI approach

Christopher Krich[1,2], Jakob Runge[3], Diego G. Miralles[2], Mirco Migliavacca[1], Oscar Perez-Priego[1], Tarek El-Madany[1], Arnaud Carrara[4], and Miguel D. Mahecha[1,5]

[1]Max Planck Institute for Biogeochemistry, 07745 Jena,Germany
[2]Laboratory of Hydrology and Water Management, Ghent University, Ghent 9000, Belgium
[3]German Aerospace Center, Institute of Data Science, 07745, Jena, Germany
[4]Fundación Centro de Estudios Ambientales del Mediterráneo (CEAM), 46980 Paterna, Spain
[5]German Centre for Integrative Biodiversity Research (iDiv), Deutscher Platz 5e, 04103 Leipzig, Germany

**Correspondence:** Christopher Krich (ckrich@bgc-jena.mpg.de)

**Abstract.** ~~Local meteorological conditions and biospheric activity~~ The dynamics of biochemical processes in terrestrial ecosystems are tightly coupled to local meteorological conditions. Understanding these ~~links~~ interactions is an essential prerequisite for predicting ~~the Earth system under climate changeconditions~~e.g. the response of the terrestrial carbon cycle to climate change. However, many empirical studies ~~on the interaction between the biosphere and the atmosphere are based~~ in this field rely on correlative approaches ~~that are not able to deduce causal paths,~~ and only very few studies apply causal discovery methods. Here ~~, we use~~ we explore the potential of a recently proposed causal graph discovery algorithm~~, which aims~~ to reconstruct the causal dependency structure underlying ~~a set of time series . We explore the potential of this method to infer temporal dependencies in~~ biosphere-atmosphere interactions. Using artificial time series with known dependencies that mimic real-world biosphere-atmosphere interactions ~~. Specifically~~ we address the ~~following questions: How do periodicity and heteroscedasticity influence causal detection rates~~influence of non-stationarities, i.e. ~~the detection of existing and non-existing links? How consistent are results for noise-contaminated data? Do results exhibit an increased information content that justifies the use of this causal-inference method? We explore the first question using artificial time series with well known dependencies that mimic real-world biosphere-atmosphere interactions. The two remaining questions are addressed jointly~~ periodicity and heteroscedasticity, on the estimation of causal networks. We then investigate the interpretability of the method in two case studies~~utilizing observational data~~. Firstly, we analyse three replicated eddy covariance datasets from a Mediterranean ecosystem~~at half hourly time resolution allowing us to understand the impact of measurement uncertainties. Secondly, we analyse~~ , and secondly, we explore global NDVI time series (GIMMS 3g) along with gridded climate data to study large-scale climatic drivers of vegetation greenness. We compare the retrieved causal graphs to simple cross correlation-based approaches to test whether causal graphs are considerably more informative. Overall, the results confirm the capacity of the causal discovery method to extract time-lagged linear dependencies under realistic settings. ~~The~~ For example, we find a complete decoupling of the net ecosystem exchange from meteorological variability during summer time in the Mediterranean ecosystem. However, cautious interpretations are needed as the violation of the method's assumptions due to non-stationarities increases the likelihood to detect false links. ~~Nevertheless, we consistently identify interaction patterns in observational data. Our findings suggest that estimating a~~ Overall, estimating directed biosphere-atmosphere ~~network at the ecosystem level can offer novel possibilities to unravel~~ networks helps unravelling complex multi-directional process interactions. Other than classical correlative approaches, our findings are constrained to a few meaningful ~~set~~ sets of relations which can be powerful insights for the evaluation of terrestrial ecosystem models.

## 1 Introduction

~~Understanding biosphere-atmosphere interactions is a prerequisite to accurately quantify feedbacks in the Earth system (Bonan, 2015). On the one hand, the~~ The terrestrial biosphere responds to ~~the~~ atmospheric drivers such as radiation intensity, temperature, vapour pressure deficit, and composition of trace gases. On the other hand, the biosphere influences the atmosphere via partitioning ~~the~~ incoming net radiation into sensible, latent, and ground heat fluxes as well as via controlling the exchange of trace gases and volatile organic compounds. Over the past decades, many of these processes have been identified and their physical, chemical and biological effects have been investigated (see e.g. Monson and Baldocchi, 2014; McPherson, 2007, for overviews). However, ~~the synergistic effects of these processes and the specific cause-effect interactions underlying these effects are still not fully understood (Baldocchi D and T., 2016; Miralles et al., 2018)~~there are still substantial unknowns regarding the exact causal dependencies among the different processes (Baldocchi D and T., 2016; Miralles et al., 2018), which leads to large uncertainties when predicting e.g. ecosystem responses to drought conditions **??**.

~~Today, there is a manifold of monitoring systems operating at various spatial and temporal scales~~Multiple ecological monitoring systems have been setup to monitor ecosystem dynamics. Networks of eddy covariance towers ~~offer high temporal resolution to study the dependence between~~ continuously monitor carbon, water, and energy fluxes ~~and the atmosphere under a variety of normal and stress conditions or in response to disturbances~~ in high temporal resolution (Baldocchi, 2014). Satellite remote sensing data complement this picture and can be used in tandem (**??**). They typically only monitor vegetation states at multi-day resolutions and some products offer nearly complete global ~~coverages~~ coverage (Justice et al., 2002; Woodcock et al., 2008). The actual and future satellite missions are leading to rapid development in the field with ever higher spatial, temporal, and spectral measurements (Malenovský et al., 2012; Guanter et al., 2015; Qi and Dubayah, 2016).

The study of biosphere-atmosphere interactions using observations typically relies on correlative approaches, or is based on model-data i.e. requires *a-priori* knowledge. ~~Only few attempts have been made to learn directional dependencies in a data-driven manner in biogeosciences. For instance, Ruddell and Kumar (2009) used transfer entropy, a bivariate information theoretic measure, to estimate networks of information flow. These networks constructed for a corn-soybean ecosystem under drought and normal conditions showed substantial differences in connectivity. The decoupling during drought between variables describing both land and atmospheric conditions was attributed to changes in the feedback patterns for the two conditions.~~ In recent years, a new branch in statistics aiming for causal inference from empirical data has experienced substantial progress. The idea of causal inference emerged already in the early 20th century (Wright, 1921). Later, Granger suggested one of the first applicable formalisms (Granger, 1969); since then, several efforts in ecology and climate science have concentrated on the bivariate form of Granger causality (Elsner, 2006, 2007; Kodra et al., 2011; Attanasio, 2012; Attanasio et al., 2012). From an information theoretic perspective transfer entropy (Schreiber, 2000) evolved as a frequently used measure to infer directionality and amount of information flow (Kumar and Ruddell, 2010; Ruddell et al., 2015; Gerken et al., 2018; Yu et al., 2019). For instance, Ruddell and Kumar (2009) used transfer entropy to estimate networks of information flow. These networks constructed for an agricultural site under drought and non-drought conditions showed substantial differences in connectivity, especially between subsystems comprising variables of land and atmospheric conditions. Those changes in connectivity are attributed to changes in the feedback patterns between the subsystems for drought and normal conditions. The original forms of both Granger causality and transfer entropy are bivariate and converge for the case of vector auto regressive models. While Granger causality is typically limited to linear relationships, transfer entropy captures also non-linear interactions, but requires very large data quantities for the estimation of the probability density function.

Aiming to mitigate some of the limitations of the traditional Granger causality, Detto et al. (2012) used a conditional spectral Granger causality framework that allows to disentangle system inherent periodic couplings from external forcing. The disentanglement is enabled via decomposition into the frequency domain using wavelet theory. This method enabled the finding that soil respiration in a pine and hardwood forested ecosystem in winter is not influenced by canopy assimilation but only by temperature, a result that would not be detectable via lagged correlation or bivariate Granger causality. A time-frequency representation of Granger causality was presented by **?** which allowed to identify anomalous events in marine and ecological time series. Green et al. (2017) used a similar approach as Detto et al. (2012) to investigate biosphere-atmosphere feedback loops. It ~~is~~ was found that they can explain up to 30% of variance in radiation and precipitation in certain regions. Recently, Papagiannopoulou et al. (2017a) applied a non-linear multivariate conditional Granger causality framework to study climatic drivers of vegetation at the global scale. This approach revealed that water ~~limitations on plant productivity play a considerably larger role than previously expected (Papagiannopoulou et al., 2017b). These examples show~~ availability dominates plant productivity as 61% of the vegetated surface appeared water limited rather than controlled by radiation or temperature (Papagiannopoulou et al., 2017b). In the case of transfer entropy, Goodwell and Kumar (2017a, b) developed a redundancy measure which allows to distinguish unique, synergistic and redundant information transfer of a bi or potentially multivariate system to a target variable. This modification enables a stronger multivariate interpretation of process networks constructed with transfer entropy. Changes in connectivity then potentially point to different ecosystem response strategies to disturbances (Goodwell et al., 2018). These examples highlight that unexpected interaction patterns can ~~be found~~ in principle be identified from data only and may challenge ~~our~~ theoretical assumptions. In fact, in the last years the science of causal inference has developed a strong theoretical foundation and several algorithms have been proposed ~~(Spirtes et al., 2001; Pearl, 2009; Peters et al.~~ However, ~~we only find few studies that test the~~ only few studies test the suitability of this latest generation of ~~such methods in ecosystem ecology (see e.g. Shadaydeh et al., 2018; Christiansen and Peters, 2018)~~ methods to understand ecosystem dynamics (see e.g. Shadaydeh et al., 2018; **?**; Christiansen and Peters, 2018).

Ecological and climate data ~~is usually~~ are often time ordered. ~~Using the concept of time series graphs (Ebert-Uphoff and Deng, 2012), the time order~~ This property can be exploited to ~~create efficient causal graph discovery algorithms (Runge, 2018a)~~ construct time series graphs (Ebert-Uphoff and Deng, 2012). Recently, ~~Runge et al. (2018) introduced such an algorithm~~ **?** introduced an algorithm to estimate such graphs, called PCMCI, a combination of the PC algorithm (named after its inventors Peter and Clark, Spirtes and Glymour, 1991) and the Momentary Conditional Independence (MCI) test. PCMCI has been successfully applied to artificial ~~tests~~ (Runge et al., 2018) and climatological case studies (Runge et al., 2014; Kretschmer et al., 2016). Hence, this method could be potentially of ~~very~~ high relevance for learning the ~~casual dependency structure in the complex~~ causal dependency structure underlying biosphere-atmosphere ~~system~~ interactions.

In this study, we explore the potential of PCMCI for disentangling and quantifying interactions and feedbacks between terrestrial biosphere state and fluxes and meteorological variables. The study is structured as follows: ~~Firstly, we describe~~ In Sect. 2 we motivate and introduce the method from an ecological perspective. We also describe artificial and real world datasets explored in this study. The results in Sect. **??** describes the performance of the method on artificial time series data with ~~well-known~~ known dependencies that mimic some basic properties of observed land surface fluxes such as heteroscedasticity~~(Sect.3.1). Secondly, we explore~~ . We then report on the exploration of three replicated eddy covariance measurement towers in a Mediterranean ecosystem and explore how the identified interdependencies of carbon and energy fluxes and micrometeorological observations vary over time~~(Sect.3.2). Thirdly, we use~~ . Further, we present the analysis of global satellite data of vegetation greenness to understand the lagged dependency of ecosystems with respect to climatic drivers~~(Sect.3.3)~~. Based on these results, ~~we discuss~~ Sect.4 discusses the potentials and limitations of PCMCI for other applications in land-atmosphere studies and give recommendations for further methodological developments~~(Sect.4)~~.

## 2 Method and Data

### 2.1 ~~Causal Discovery via PCMCIPCMCI assesses the causal structure of a~~ From bivariate to multivariate ~~dataset or~~ measures of causality

Monitoring an ecosystem with continuous observations of net ecosystem exchange (NEE), the underlying gross primary production (GPP) and ecosystem respiration ($R_{textnormaleco}$) together with the relevant drivers i.e. global radiation (Rg), surface air temperature (T), and soil moisture (SM), allows to study the dynamics of the carbon cycle in terrestrial ecosystems. To foster its understanding, a fundamental question is how these variables causally depend on each other. This requires the identification of directional dependencies such as the well known effects of SM → GPP and GPP → $R_{eco}$ and their differentiation from physically implausible links such as $R_{eco}$ → GPP. Graphical causal models (Spirtes et al., 2001) provide a framework to represent and identify causal relations based on conditional independence relations in data streams of this kind. In the case of an ecological monitoring site as described here, we can exploit the temporal information of the observations for identifying a time series graph as a type of graphical model (Runge, 2018a). Formally this can be stated as follows: The variables $X^i_t$ comprise a multivariate stochastic process $\mathbf{X}$ ~~by estimating its time series graph. In short, the nodes of a~~ (where i is the variable index, in the example $i \in \{\mathrm{Rg}, \mathrm{T}, \mathrm{GPP}, \mathrm{R}_{eco}, \mathrm{SM}\}$, and t is the time index). A time series graph $\mathcal{G}$ ~~represent single variables $X^1, X^2, ... \in \mathbf{X}$ at specific (lagged) time steps $t, t-1, .., t-\tau_{max}$. A lag is the number of time steps~~ visualizes how the individual variables $X^i \in \mathbf{X}$ depend on each other at specific time lags $\tau$ ~~between two nodes $X^i_{t_1}$~~, i.e. $X^i_{t-\tau}$ with $\tau \in \{1, .., \tau_{max}\}$ (see Runge, 2018a, for definitions). In the following, we refer to a variable $X^i_{t-\tau}$ that is causally affecting a variable $X^j_t$ as 'parent' or 'driver' and the latter as 'receiver' or 'target'. To come to a causal interpretation, it is important to exclude dependencies between two variables that are due to common drivers ($X^i_{t-\tau_1} \leftarrow X^s_{t-\tau_2} \rightarrow X^j_t$) or indirect paths ($X^i_{t-\tau_2} \rightarrow X^s_{t-\tau_1} \rightarrow X^j_t$). For instance, when estimating the effects of GPP on $R_{eco}$ and Rg on $R_{eco}$ using a bivariate measure, one likely obtains implausible results like to strong or even unexpected links because T, respectively as the common driver and mediator (indirect path), is not accounted for. To exclude dependencies due to common drivers or indirect paths, conditional independence tests are used, denoted as $CI(X^i_{t-\tau}, X^j_t|\mathcal{S})$, with some conditioning set $\mathcal{S}$. If any variable (or their combination) in $\mathcal{S}$ explains the dependence between $X^i_{t-\tau}$ and ~~$X^j_{t_2}$~~ $X^j_t$, then the CI statistic is zero.

Two prominent methods that aim for directional dependencies are Granger causality and transfer entropy (Granger, 1969; Schreiber, 2000 Granger causality is typically estimated as a vector autoregressive model and thus captures only linear links. Transfer entropy, based on information theory, captures also non linear dependencies. It can be shown that for multivariate Gaussians, transfer entropy is equivalent to Granger causality (**?**). Both can be phrased as testing for conditional independence (Runge et al., 2019). In their original bivariate form, neither of these two methods accounts for third variables. But both can also be extended to deal with multivariate time series as required here (Runge et al., 2012b; Granger, 1969). There are even non-linear and spectral modifications of Granger causality which have been applied to study biosphere atmosphere interactions (Papagiannopoulou et al., 2017a; D However, the estimation of multivariate transfer entropy is challenging due to the "curse of dimensionality" (Runge et al., 2012b) and also multivariate Granger causality exhibits low link detection power for larger number of variables (higher dimensions) and limited sample size, as is the case in our application (**?**). The strong decrease in detection power happens when using the whole past $\mathbf{X}_t^- = (\mathbf{X}_{t-1}, \mathbf{X}_{t-2}, ...)$ of $X_t^j$, truncated at a maximum lag $\tau_{max}$, as a conditioning set $\mathcal{S}$. The problem is that this set can contain a high number of conditions which are irrelevant. For example, when assessing the effect of Rg at a specific time lag $\tau$ on GPP using multivariate Granger causality one would create a vector auto regressive model comprising all variables, i.e. ~~$\tau = t_1 - t_2$ for $t_1 > t_2$. To generate a causal graph~~ Rg, T, SM, GPP and $R_{eco}$ at each available lag. But $R_{eco}$, dominated by heterotrophic respiration, is not expected to affect gross primary productivity and could be removed to decrease the dimensionality. However, manually selecting conditions is not desirable when the underlying dependence structure is unknown which is why ideally the conditioning set is identified automatically.

PCMCI addresses this issue by reducing the set of conditions $\mathcal{S}$ prior to quantifying the dependence between two variables. The two-step approach utilizes a variant of the PC algorithm (Spirtes and Glymour, 1991) and the momentary conditional independence measure (MCI) (**?**). More detailed descriptions are given in Sect. 2.4 and 2.5, respectively (full description of PCMCI including proofs and quantitative comparisons with other methods are provided in **?**). A schematic of the PCMCI approach is given in Fig. A1. PCMCI belongs to the family of causal graphical models (Spirtes et al., 2001; Pearl, 2009), and follows the assumptions listed in Sect. 2.2. In the limit of infinite time series length, PCMCI converges to the true graph of dependencies, which is why we use the term “causal”. As we deal with finite sample length and partially unfulfilled assumptions, spurious links can still appear (beyond the expected false positive rate) and therefore each detected link has to be interpreted with caution.

### 2.2 Assumptions

PCMCI assesses the causal structure of a multivariate dataset or process $\mathbf{X}$ by estimating its time series graph. To draw causal conclusions from observational data~~through statistical dependencies, a series of assumptions must be adopted. Here, we assume:~~ , any causal method must adopt a number of assumptions (Pearl, 2009; Spirtes et al., 2001). For the time series case, here we assume time order, the causal Markov condition, faithfulness, causal sufficiency, causal stationarity, and no contemporaneous causal effects (Runge et al., 2018). PCMCI is applied in combination with the ParCorr linear independence test based on partial correlations (cf. Sect. 2.3). This application additionally requires stationarity in mean and variance and linear dependencies. In the following, we briefly discuss these assumptions ~~(further details in Runge, 2018a) and refer to a variable $X^i$ that is causally affecting a variable $X^j$ as 'parent' or 'driver' and the latter as 'receiver' or 'target'~~(further details in Runge, 2018a; **?**).

The time order within the time series allows to orient directed links which are only pointing forward in time. This accounts for causal information propagating forward in time only, i.e. the cause shall precede the effect. Therefore, a directed causal link $X_{t_1}^i \to X_{t_2}^j$ can only exist between two nodes $X_{t_1}^i, X_{t_2}^j$ if $t_1 < t_2$. When a contemporaneous link is found, i.e. $t_1 = t_2$, it is considered to be undirected. ~~The connection between the graph $\mathcal{G}$ and its process $\mathbf{X}$ is given by the causal Markov condition together with the faithfulness. The Markov condition says that if there is no link in the graph, there is conditional independence in the distribution, and if there is no conditional independence, there is connectedness in the graph; the reverse relations, if there is conditional independence, there is also separation in the graph and if there is connectedness in the graph, there is no conditional independence, are given by the faithfulness assumption. With these assumptions the graph is a visualisation of the conditional dependence and independence relationships among the variables including their lags. Finally, the~~ In ecological language it means that in order to claim that Rg is driving GPP any change in Rg that is affecting GPP must be measured at a time step before the change in GPP occurs. The Causal Markov and faithfulness assumptions relate the underlying physical causal mechanisms to statistical relationships manifest in the data. The Causal Markov condition states that if two processes are not directly connected by some physical mechanism, then they should be statistically independent conditional on their direct drivers, like Rg and $R_{eco}$ conditional on T . The faithfulness assumption concerns the other direction: if two processes are statistically independent, then there cannot be a direct physical mechanism. The causal sufficiency assumption implies that ~~,~~ every common cause of two or more variables $X^i \in \mathbf{X}$ is included in $\mathbf{X}$. If this is not the case, detected links may be indirect or due to an unobserved common driver. However, the absence of a link in the detected graph still implies that no direct link is present (as this only requires the assumption of faithfulness).

~~Several causality methods suffer from high dimensionality, i.e. multivariate transfer entropy (Runge et al., 2012b). They use the whole past $\mathbf{X}_t^- \setminus X_{t-\tau}^i$ of $X_t^j$ with $\mathbf{X}_t^- = (\mathbf{X}_{t-1}, \mathbf{X}_{t-2}, ...)$ as a conditioning set $\mathcal{S}$ in the estimation of the test statistic $I(X_{t-\tau}^i, X_t^j|\mathcal{S}) : \mathcal{S} = \mathbf{X}_t^- \setminus X_{t-\tau}^i$. PCMCI addresses this issue by reducing the set of conditions $\mathcal{S}$.PCMCI first estimates $\mathcal{S}$ for each $X_t^j$. The estimation removes all variables that are either independent or dependent due to indirect paths or common drivers only and leaves only relevant conditions converging to the true causal parents in the limit of infinite sample size. This is done using a variant of the PC algorithm (Spirtes et al., 2001). The conditioning set is subsequently used in the MCI step to test every possible link; MCI also attributes a link strength. These two steps as well as the concept of independence tests, which are at the core of both PC and MCI algorithms, are explained in more detail in the following~~For example, Rg is expected to influence $R_{eco}$ via T, the indirect path. Though, a link between Rg and $R_{eco}$ might be detected if T is not included in the analysis. However, a missing link between T and $R_{eco}$, might indicate conditions inhibiting respiratory processes, i.e. very cold temperatures with frozen surfaces or very dry conditions with dead vegetation coverage. Causal stationarity refers to the existence of links over time. In a deciduous forest, for example, the ecosystem's $CO_2$ exchange is not causally stationary as the link Rg $\rightarrow$ GPP is given in summer but not in winter. Formally, a process $\mathbf{X}$ with graph $\mathcal{G}$ is called causally stationary over a time index $\mathcal{T}$, if and only if for all links $X_{t-\tau}^i \rightarrow X_t^j$ in the graph the condition $X_{t-\tau}^i \not\perp\!\!\!\perp X_t^j \mid \mathbf{X}_t^- \setminus \{X_{t-\tau}^i\}$ holds for all $t \in \mathcal{T}$.

### 2.2.1 ~~Independence Test~~

## 2.3 Independence Test

At the core of PCMCI ~~,~~ there are conditional independence tests $CI(X_{t-\tau}^i, X_t^j, \mathcal{S})$ ~~testing for~~ to evaluate whether $X_{t-\tau}^i \perp\!\!\!\perp X_t^j \mid \mathcal{S}$ given a conditioning set $\mathcal{S}$. Within the PCMCI software package Tigramite (Runge, 2018b), several independence tests are implemented. Here, we focus on the linear independence test called ParCorr. The ParCorr conditional independence test is based on partial correlations and a t-test. This assumes the model

$$X^i = \mathcal{S}\beta_{X^i} + \epsilon_{XX^i}, \quad YX^j = \mathcal{S}\beta_{X^j} + \epsilon_{YX^j}, \tag{1}$$

with coefficients $\beta$ and Gaussian noise $\epsilon$. This leads to the residuals

$$r^{xX^i} = X - X^i - \mathcal{S}\hat{\beta}_{X^i}, \quad r^{yX^j} = Y - X^j - \mathcal{S}\hat{\beta}_{X^j} \tag{2}$$

with estimated $\hat{\beta}$. ParCorr removes the influence of $\mathcal{S}$ on ~~X and Y~~ $X^i$ and $X^j$ via ordinary least squares regression and tests for independence of the residuals using the Pearson correlation with a t-test. The independence test returns a ~~p-value~~ $p$-value and test statistic value $I$, i.e. the correlation coefficient in case of ParCorr. Thus, to identify the effect of GPP on $\mathrm{R}_{\mathrm{eco}}$ that does account for their common driver $\mathrm{T} \in \mathcal{S}$, ParCorr will perform a linear regression of T on both GPP and $\mathrm{R}_{\mathrm{eco}}$ accounting for time lags. The p-value of the residuals' partial correlation test can be used to assess whether the two variables are dependent.

### 2.3.1 ~~PC algorithm~~

## 2.4 PC algorithm

~~The PC algorithm estimates a set of parents for each variable of the process $X_t^j \in \mathbf{X}_t$ which are used as low-dimensional conditions in the MCI algorithm. A comprehensive pseudo code~~ To efficiently estimate $CI(X^i_{t-\tau}, X^j_t|\mathcal{S})$ the conditioning set $\mathcal{S}$ should be as small as possible which means that it should only contain relevant conditions, which allow to isolate the unique influence of $X^i_{t-\tau}$ on $X^j_t$. For an estimation of $CI(\mathrm{Rg}_{t-\tau},\mathrm{GPP}_t|\mathcal{S})$, for example, $\mathcal{S}$ should contain T and SM (at certain lags), as they influence the ability of an ecosystem to perform photosynthesis. Likewise, when estimating $CI(\mathrm{T}_{t-\tau},\mathrm{GPP}_t|\mathcal{S})$, $\mathcal{S}$ should include Rg and SM for the same reasons. A sufficient set of relevant conditions includes the drivers/parents of the variable $X^j_t$. Consequently, the aim of the PC step is to identify an as small as possible superset of the parents of each variable included in the process. The algorithm uses a variant of the PC algorithm (Spirtes et al., 2001); a comprehensive pseudo-code of this procedure is given in ~~Runge et al. (2018). The algorithm starts with a fully connected graph and iteratively removes links if conditional independence is found. At first, a preliminary set of parents $\widetilde{\mathcal{P}}$ for each $X^j_t$ equal to~~ the supplementary materials of **?**. In the limit of infinite sample size the relevant conditions indeed converge to the true causal parents, practically though, an estimate that contains a few irrelevant conditions, like $\mathrm{R}_{\mathrm{eco}}$, is sufficient as well.

The PC step starts by initializing the whole past of ~~the process $\mathbf{X}_t$ is initialised~~ a process: $\widetilde{\mathcal{P}}(X^j_t) = \mathbf{X}^-_t = \{X^i_{t-\tau} : i = 1,...,N, \tau = 1,...,\tau_{max}\}$. Next, ~~conditional independence $X^i_{t-\tau} \perp\!\!\!\perp X^j_t \mid \mathcal{S}$ is tested for all $X^i_{t-\tau} \in \widetilde{\mathcal{P}}$~~ by evaluating $CI(X^i_{t-\tau}, X^j_t, \mathcal{S})$, conditions $X^i_{t-\tau}$ are removed from $\widetilde{\mathcal{P}}(X^j_t)$ that are independent of $X^j_t$ conditionally on a subset $\mathcal{S} \in \widetilde{\mathcal{P}}(X^j_t)\setminus\left\{X^i_{t-\tau}\right\}$. $\mathcal{S}$ ~~is a subset of $\widetilde{\mathcal{P}}(X^j_t)\setminus\left\{X^i_{t-\tau}\right\}$~~ starts as the empty set $\emptyset$ and is iteratively increased. For instance, let $X^i_{t-\tau}$ be $\mathrm{R}_{\mathrm{eco}}$ (at a specific lag) and $X^j_t$ be GPP. The conditional independence ~~test is embedded into two loops. The outer loop iteratively increases the cardinality $p$ of $\mathcal{S}$ starting from 0, the empty set. Thus it is first tested, whether $X^i$ and $X^j$ are independent. Further, only the p strongest conditions are selected. The inner loop iterates through all $X^i_{t-\tau} \in \widetilde{\mathcal{P}}(X^j_t)$. The cardinality is increased until $|\mathcal{S}| = |\widetilde{\mathcal{P}}(X^j_t)\setminus\left\{X^i_{t-\tau}\right\}| - 1$. At the end of each iteration in~~ between GPP and $\mathrm{R}_{\mathrm{eco}}$ will be estimated first by using no conditions. If GPP and $\mathrm{R}_{\mathrm{eco}}$ appear related, one variable will be included in the conditioning set. If the residuals are still dependent, a second variable is included and so on. When T is part of the conditioning set, the ~~outer loop the non-significant parents are removed from $\widetilde{\mathcal{P}}(X^j_t)$.~~ residuals of GPP and $\mathrm{R}_{\mathrm{eco}}$ might not be dependent anymore and $\mathrm{R}_{\mathrm{eco}}$ is removed from the estimated set of parents of GPP. The PC algorithm adopted in PCMCI efficiently selects those conditioning sets to limit the number of tests conducted.

Every conditional independence test is evaluated at a significance threshold ~~called~~ $\alpha_{pc}$, which is usually set to a liberal value between 0.1 and 0.4. Alternatively, in tigramite one can let $\alpha_{pc}$ unspecified. PCMCI then evaluates the best choice of $\alpha_{pc} \in \{0.1, 0.2, 0.3, 0.4\}$ based on the Akaike information criterion which is further explained in (Runge et al., 2018).

### 2.4.1 ~~MCI tests~~

## 2.5 MCI tests

MCI is the actual causal discovery step that ascribes a ~~p-value~~ $p$-value and strength to each possible link. MCI iterates through all pairs $(X^i_{t-\tau}, X^j_t) : i = 1,...,N,\ \tau = 0,...,\tau_{max}$ and calculates ~~$\mathrm{CI}(X^i_{t-\tau}, X^j_t, \mathcal{S})$.~~ $CI(X^i_{t-\tau}, X^j_t, \mathcal{S})$ where $\mathcal{S}$ consists of the two ~~potentially multivariate~~ (super-)sets of parents $\widetilde{\mathcal{P}}(X^j_t)$ and $\widetilde{\mathcal{P}}(X^i_{t-\tau})$ obtained in the PC step. $\widetilde{\mathcal{P}}(X^i_{t-\tau})$ is constructed by shifting the time series of $\widetilde{\mathcal{P}}(X^i_t)$ by $\tau$. In case $X^i_{t-\tau} \in \widetilde{\mathcal{P}}(X^j_t)$, $X^i_{t-\tau}$ has to be removed from $\widetilde{\mathcal{P}}(X^j_t)$. If $\tau = 0$, conditional dependence is estimated for contemporaneous nodes $X^j_t$ and $X^i_t$. Due to missing time order, a dependence would be left undirected. Further, as the parents $\widetilde{\mathcal{P}}(X^i_t)$ and $\widetilde{\mathcal{P}}(X^j_t)$ used in each conditional dependence test are defined to lie in the past of $X^i_t$ and $X^j_t$, links, both contemporaneous and lagged, can be spurious due to contemporaneous common drivers or contemporaneous indirect paths. The absence of a link, though, means that a physical (contemporaneous) link is unlikely (assuming faithfulness, cf. Runge et al. (2018)). For simplicity, the previously given examples were omiting the time lag. Thus if $R_{eco}$ responds instantaneously (considering the sampling temporal resolution) to changes in T but T responds with a time lag to Rg, both variables will likely appear contemporaneously coupled to Rg.

The link strength ~~is~~ in the PCMCI framework can be given by the effect size of the conditional independence test statistic measure ~~CI~~ $CI$ used in combination with MCI. In case of ParCorr, the effect size is given by the partial correlation value, which is between -1 and 1. ~~This~~ Assuming a linear Gaussian model the partial correlation value is shown ~~in Runge et al. (2014)~~ to directly depend on the receiver's and driver's variance as well as the coupling coefficient ~~. Even~~ (Runge et al., 2019):

$$\rho^{MCI}_{X^i_{t-\tau}\to X^j_t} = \frac{c\,\sigma_{X^i_{t-\tau}}}{\sqrt{\sigma^2_{X^j_t} + c^2\sigma^2_{X^i_{t-\tau}}}} \tag{3}$$

where $\sigma_{X^i_{t-\tau},X^j_t}$ are the variances of the noise/innovation terms driving $X^i_{t-\tau}$ and $X^j_t$, respectively, and $c$ is their coupling coefficient. In practice, also non-linear links can ~~be~~ often be well detected with ParCorr ~~as they can often~~ in so far they be linearly approximated. In case the linear part is even ~~stronger~~ "stronger" than the non-linear part, ParCorr ~~can have better detection rate~~ might also have a better detection power than a non-linear independence test (Runge et al., 2018).

## 2.6 Data

### 2.6.1 Artificial Dataset - Test Model

We tested the algorithm on artificial datasets prior to its application to real world data. ~~Using~~ The artificial dataset was created using a test model which takes time series of measured global radiation ($\mathcal{R}g$) ~~we created~~ and creates three artificial time series that conceptually represent temperature ($\mathcal{T}$), gross primary production ($\mathcal{GPP}$) and ecosystem respiration ($\mathcal{R}eco$). Note that this test model is not intended to accurately represent observed land-atmosphere fluxes, but only serves to test the procedure. The model incorporates one linear auto dependence $\mathcal{T}_{t-\tau_1} \to \mathcal{T}_t$, one linear additive cross-dependence $\mathcal{R}g_{t-\tau_2} \to \mathcal{T}_t$ and two non-linear dependencies, multiplicative $\mathcal{R}g_{t-\tau_3} \bullet \mathcal{T}_{t-\tau_4} \to \mathcal{GPP}_t$, and multiplicative exponential $\mathcal{GPP}_{t-\tau_5} \bullet c^{\mathcal{T}_{t-\tau_6}} \to \mathcal{R}eco_t$ (cf. Fig. 1) according to the equations:

$$\mathcal{R}g_{mo} = \mathcal{R}g_{obs} \tag{4}$$

$$\mathcal{T}_{mo}(t) = c_1\, \mathcal{T}_{mo}(t-\tau_1) + c_2\, \mathcal{R}g_{mo}(t-\tau_2) + \xi_T \tag{5}$$

$$\mathcal{GPP}_{mo}(t) = c_3\, \mathcal{R}g_{mo}(t-\tau_3) * \mathcal{T}_{mo}(t-\tau_4) + \xi_{GPP} \tag{6}$$

$$\mathcal{R}eco_{mo}(t) = c_4\, \mathcal{GPP}_{mo}(t-\tau_5) * c_5^{\frac{\mathcal{T}_{mo}(t-\tau_6)-T_{ref}}{10}} + \xi_{\mathcal{R}eco} \tag{7}$$

The parameters $c_1$, $c_2$, ..., $c_5$ are referred to as coupling coefficients, and the time lags are noted as $\tau_1$, $\tau_2$,..., $\tau_5$. The subscripts $_{mo}$ and $_{obs}$ abbreviate model and observation, respectively. $T_{ref}$ is set to 15°C. The term $\xi$, termed "intrinsic" or "dynamical noise", here represents values from uncorrelated, normally distributed noise. Having dynamic noise is essential for a method utilizing conditional independence tests. It is based on the assumption that a process or state is never fully described by its deterministic part because there are unresolved intrinsic processes, summarized as $\xi$.

The model was fitted to real observational data (using radiation, temperature and land-atmosphere fluxes) of daily time resolution, measured by the eddy-covariance method (Baldocchi et al., 1988; Baldocchi, 2003) from FLUXNET, by minimizing the sum of squared residuals using the gradient descent implemented in the `Optim.jl` package (Mogensen and Riseth, 2018). We fitted the model to 72 sites listed in Table B1 given in the Supplementary Material section. The value range for the coupling coefficients $c_1$ to $c_4$ and $c_5$ were set to [0.2,1] and [1,2.5], respectively. The lags were limited to integer values in the range [0,25]. ~~For the fitting, the dynamical noise $\xi$ was set to 0.~~ The distributions of obtained lags and coupling coefficients are given in the Supplementary Material Fig. B1 to E1. The fitting process thus generated 72 sets of parameters, containing coupling coefficients and lag values, which were used for the time series generation.

From each of the 72 sets of parameters we generated four sets of time series each having a length of 500 years. The time series generation was initiated using two types of data: first, uncorrelated, normally distributed noise, and second, unprocessed radiation data as used during the fitting (the available radiation data was repeated to 500 years). The resulting datasets are called baseline dataset and seasonality dataset, respectively. In both cases, the model was run twice, once with homoscedastic (constant variance of $\xi$), once with heteroscedastic dynamical noise $\xi$. To induce heteroscedasticity, $\xi$ was multiplied with a mean daily variance that was extracted for each variable at each FLUXNET site. In Supplementary Material Fig. F1 a five year time series excerpt from Hainich site (Knohl et al., 2003b) is shown. A third dataset is generated by anomalization (subtraction of smoothed seasonal mean) of the seasonality dataset.

### 2.6.2 Eddy Covariance Data - Majadas de Tiètar Experimental site

Data from three towers located in Majadas de Tiètar, (ES-LMa, ES-LM1, ES-LM2), a Mediterranean Savanna in central Spain, are used (coordinates of central tower: 39°56'25"N 5°46'29"W). Meaurements include the exchange of $CO_2$ between the land surface and atmosphere at half-hourly resolution using the eddy covariance method. The three tower footprints received different fertilisation treatments in spring 2015 (El-Madany et al., 2018). We consider data from before the fertilization from April 2014 to March 2015 of shortwave downward radiation (Rg), air temperature (T), net ecosystem exchange (NEE), vapour pressure deficit (VPD), sensible heat (H) and latent heat (LE). The average temperature within this period was 17.3°C, with a total precipitation of 765mm. Most precipitation fell between October and April.

We expect the causal imprints in the data to vary between seasons and during the course of the day. To satisfy causal stationarity, we estimate networks separately for each month and consider only samples for which the potential radiation was above $\frac{4}{5}$ of the potential daily maximum, which corresponds to midday samples. We used a mask type that limits only the receiver variable to the respective month and day time values (cf. Table A1 for PCMCI parameter settings). This setting causes time series lengths ranging from 239 datapoints in December to 372 datapoints in July. Minimal and maximal lags were set to 0 and 8, respectively. ~~Due to the limited number of years, we~~ We left the data unprocessed, i.e. we did not subtract a seasonal mean for anomalisation. Constraining the samples to separate month and midday values reduces the effect of seasonality as a common driver that would lead to spurious links. Furthermore, to correct for multiple testing we applied the Benjamini-Hochberg false discovery rate correction (Benjamini and Hochberg, 1995). Thereby, the ~~p-values~~ $p$-values for the whole graph obtained from the MCI step are adjusted to control the number of false discoveries (Runge et al., 2018). We chose a two-sided significance level of 0.01.

### 2.6.3 Gridded global data set

The second observational case study was performed on a global data set. We used data with 0.5° spatial and monthly temporal resolution from 1982 to 2008. The dataset is composed of three climatic variables, global radiation (Rg), temperature (T) and precipitation (P), and one vegetation state index, the Normalized Difference Vegetation Index (NDVI). Both temperature and precipitation datasets were taken from the Climate Research Unit (CRU), version TS3.10 (Harris et al., 2014). The radiation data stems from the Climate Research Unit and National Centers for Environmental Prediction dataset (CRUNCEP, Viovy, 2016). The used NDVI data stems from the Global Inventory Monitoring and Modeling Systems (GIMMS) in version 3g_v1 (Pinzon and Tucker, 2014).

To examine the influence of radiation, temperature, and precipitation on NDVI by means of PCMCI we used the following settings. We compute the anomalies by subtracting a smoothed seasonal mean. A maximal time lag of three months was chosen based on the largest lag with significant partial correlation among all pairs of variables, partialling out only the autocorrelation of each variable. The receiver variable was limited to the growing season defined by T>0 and NDVI>0.2, which allows good comparison to Wu et al. (2015). The significance level ($\alpha_{pc}$) in the condition selection phase (cf. Sect. 2.4) was chosen based on the AIC selection criterion. A concise list of PCMCI parameters that were altered from default settings is given in Table A1.

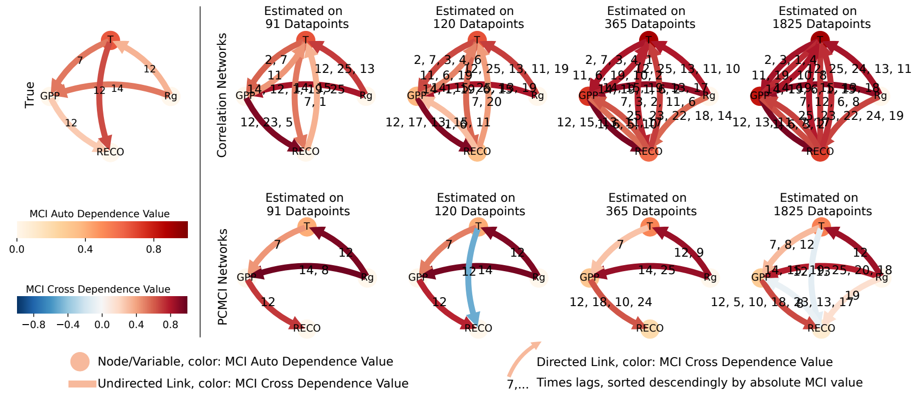


**Figure 1.** The artificial datasets are generated with a prescribed interaction structure (True Network), which is obtained by fitting the test model to the FLUXNET sites. Here we show for four time series ~~length~~ lengths the process graphs estimated via both lagged correlation and PCMCI. The data used stems from the homoscedastic realisation of the seasonality dataset of the Hainich site. The significance level was set to 0.01. The number of time lag labels were limited to five in the correlation networks. But for the longest time series typically the whole range of lags (0-25) was significant.

## 3 Results

### 3.1 Test Model

As motivating example, in Fig. 1 we show PCMCI and lagged correlation networks in the form of process graphs. It is clearly visible, that many more spurious links pass the significance threshold of 0.01 using lagged correlation as compared to using PCMCI. Those spurious links can complicate the analysis or lead to false ~~assumptions~~ conclusions and misleading hypotheses. We examined four cases of different time series lengths: 91 [183<=doy<=274] and 120 [153<=doy<=274] days, 1 and 5 years for daily data (doy: day of the year). For each time series length and each parameter set, the causal network structure was estimated for 100 realisations of the model (each based on a realization of intrinsic noise), which allowed the estimation of false positive (FPR) and true positive (TPR) detection rates. The detection rates are calculated for each tower, FPR in general and TPR link-wise. The TPR for each link is its sum of detections among 100 realisations divided by 100. The FPR is the number of falsely detected links divided by the number of all possible false links and 100. The summary of the experiments i.e. the overall false positive rate (FPR) and the distributions of the link's true positive rate (TPR) across sites are given in Fig. 2 and 3, respectively. The blue violin plots always report the case of normal distributed (non heteroscedastic) intrinsic noise and the corresponding orange violin plots summarize the case of heteroscedastic noise. The effect of heteroscedasticity and seasonality is then assessed by comparing the distributions obtained from the baseline dataset to the results of the seasonality dataset.

The FPR of homoscedastic time series in the baseline dataset is in the expected range of 0.01, the chosen significance level, indicating a well calibrated test due to fulfilled assumptions. The assumption of stationarity is violated as soon as heteroscedas-

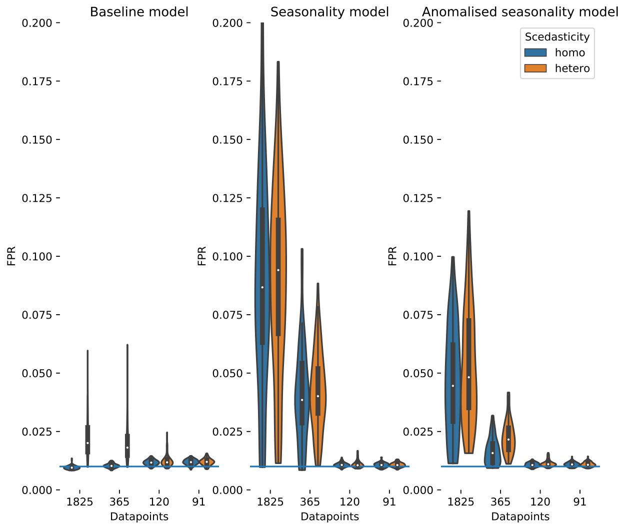


**Figure 2.** The distribution of false positive detection rates estimated for the baseline dataset, the seasonality dataset and the anomalised seasonality dataset (mean seasonal cycle subtracted). The distributions are given for different time series length (number of datapoints). Additionally, the distributions are split to show the impact of heteroscedastic noise (orange) compared to normal distributed noise (blue). The significance level of 0.01 is given by a blue horizontal line.

ticity or seasonality is present. The effect on the FPR is an increase above 0.01 for time series length of 1 and 5 years with a much stronger increase due to seasonality (factor of 4 and 8, respectively) than for heteroscedasticity (factor of 2).

The effect of non-stationarities on the TPR differs among the links. The detection of linear links ($\mathcal{R}g \rightarrow \mathcal{T}$ and $\mathcal{T} \rightarrow \mathcal{T}$) is not affected by seasonality and slightly improves for heteroscedastic dynamical noise. The detection of non-linear links is improved by seasonality with the strongest effects in the link $\mathcal{T} \rightarrow \mathcal{GPP}$. The link $\mathcal{T} \rightarrow \mathcal{R}eco$ has a ~~stonger~~ stronger non-linearity and therefore the detection rate shows a weaker effect on seasonality. Furthermore, the coupling coefficient $c_5$, the base of T, can be close to or be exactly one (cf. Fig. C1). This would actually cause on the one hand the effect of $\mathcal{T} \rightarrow \mathcal{R}eco$ to vanish, rendering a detection impossible and on the other hand result in a linear dependence of $\mathcal{GPP}$ on $\mathcal{R}eco$ which improves its detection. Heteroscedasticity seems to have a slight negative effect on non-linear links. In general, the TPRs in the seasonality dataset are quite high, even for non-linear links, and predominantly above 80% and often reaching 100%.

Comparing the TPRs of the non-linear links ~~,~~ shows some disparity. The links $\mathcal{T} \rightarrow \mathcal{GPP}$ and $\mathcal{T} \rightarrow \mathcal{R}eco$ experience zero detection in the baseline dataset but partially considerable rates in the seasonality dataset with a strong dependence on the time series length. On the contrary, the median of the TPR of the links $\mathcal{R}g \rightarrow \mathcal{GPP}$ and $\mathcal{GPP} \rightarrow \mathcal{R}eco$ is above 95% in the seasonality dataset, even for time series length as short as 91 days, but remains high in the baseline dataset. The removal of the seasonal cycle keeps the TPRs largely unaffected, but reduces the FPR. Nevertheless, it still remains above the significance level by a factor of four and two for five and one year time series length, respectively.

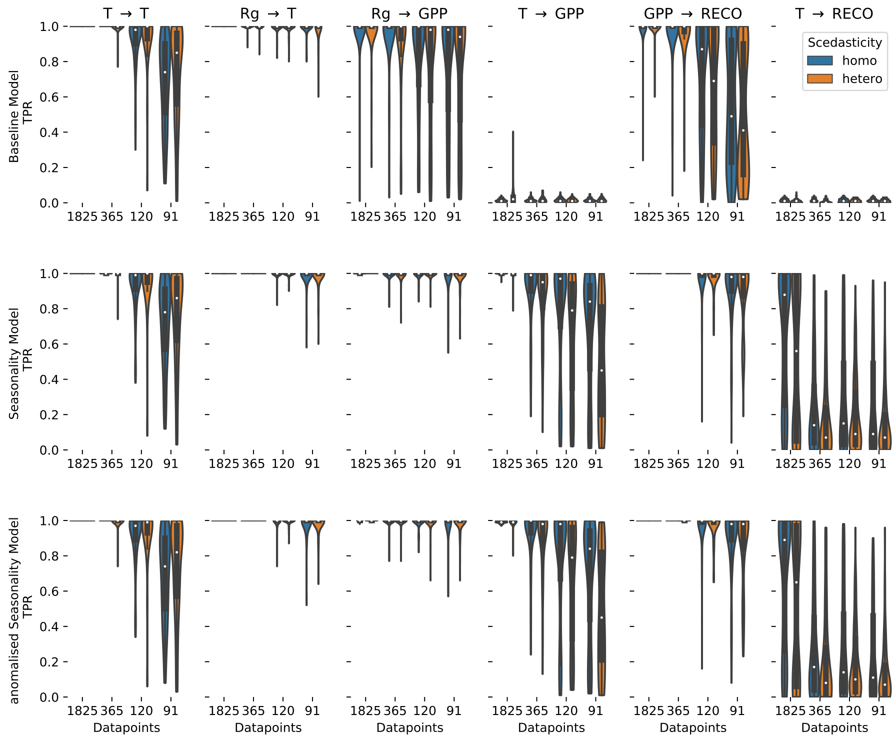


**Figure 3.** The distribution of the true positive detection rates for each link in the test model estimated for the baseline dataset, the seasonality dataset, and the anomalised seasonality dataset. The distributions are given for different time series length (number of datapoints). Additionally the distributions are split to show the impact of heteroscedastic noise (orange) compared to normally distributed noise (blue).

In summary, the seasonality dataset exhibits high TPR even for non-linear links. Compared to stationary time series, the detection of non-linear links actually benefits from seasonality. The high detection, though, comes at the cost of a high false positive rate for time series length of and above one year. To a certain degree, the increase in FPR can be counteracted by anomalization.

### 3.2 Majadas de Tiètar dataset

At first we look at the link consistency by comparing networks that were obtained for each tower within a month. The comparison is done for two months with strongly differing climate conditions: April and August. In Fig. 4 we compare the estimated link strengths (effect size estimated via partial correlation) as long as the corresponding links are significant in at least one network. The confidence intervals are overlapping for the majority of links, suggesting that the uncertainty of the fluxes is much smaller than the observed effects (El-Madany et al., 2018). Exceptions are found for only a few links (Rg$\xrightarrow{0}$T, Rg$\xrightarrow{1}$LE, VPD$\xrightarrow{1}$VPD, H$\xrightarrow{2}$H, NEE$\xrightarrow{0}$LE, H$\xrightarrow{2}$NEE, NEE$\xrightarrow{4}$NEE, number above the arrow indicates the lag) where the detection rates do not or barely overlap. Cross links (a link from one variable to another) with two or more significant appearances are predomi-

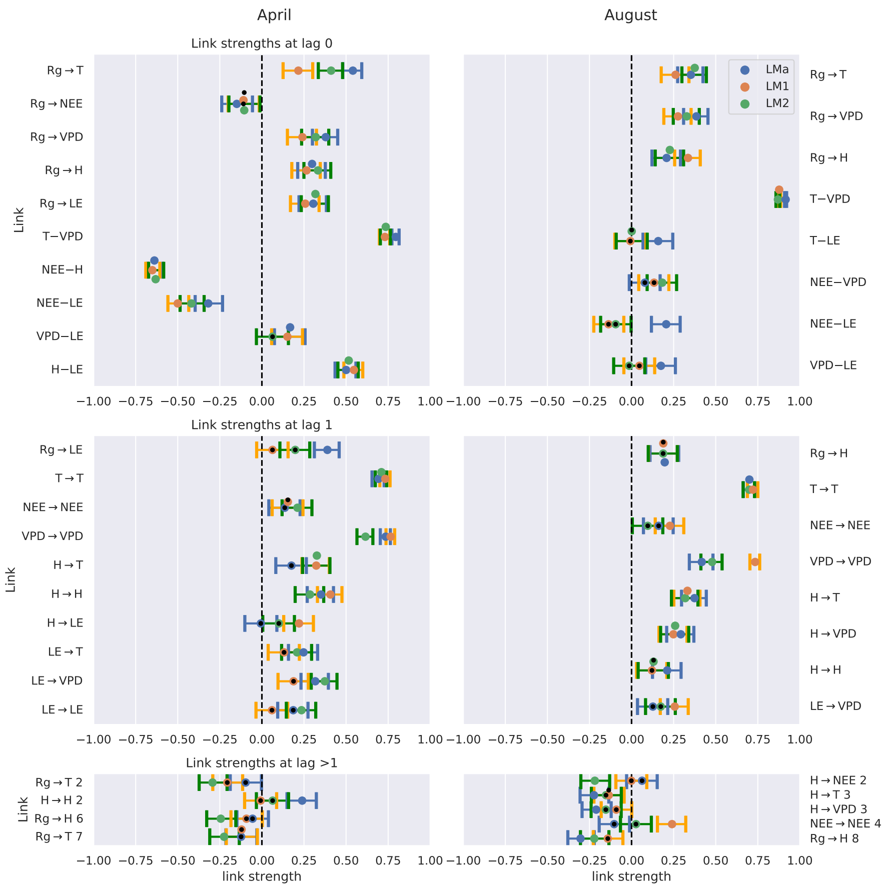


**Figure 4.** Comparison of the networks of three eddy covariance measurement stations (LMa, LM1, LM2) located in Majadas (Spain). Links that are found to be significant in one of the three networks are included. For each link, the calculated strength of all three networks is plotted with its 90% confidence interval. The colors blue, orange, and green correspond to the towers LMa, LM1, and LM2, respectively. The significance threshold is 0.01. If a link does not pass the significance, it is marked by a black dot. The links are grouped into lag 0 (top), lag 1 (middle) and all lags greater than 1 (bottom). Negative NEE is associated with carbon uptake by the ecosystem. Links at lag 0 are left undirected (−), yet as Rg is set as main driver, links incorporating Rg at lag 0 are directed (→).

nantly at zero lag. Approximately half of the links with lag one are auto-dependent links (a link from the past of a variable to its present). Comparing the links between the month April and August, distinct differences can be noticed. First, August has slightly fewer significant links compared to April. Second, the only links remaining that are significant in two or three towers are between atmospheric variables. Third, the remaining link strengths tend to be weaker in August than in April.

The difference among the seasons is further investigated in Fig. 5 which shows process graphs for each month of the year. We combine the networks of the three towers to one process graph by plotting every link that is significant in at least one tower. The process graphs in Fig. 5 visualize clearly gradual changes within the interaction structure of the biosphere-atmosphere system during the course of a year. During the main growing season from February to May, NEE is coupled strongly to the energy fluxes latent (LE) and sensible heat (H). These connections weaken, disappear or even switch sign with start and course of the dry season. Less regularly NEE also shows connections to radiation (Rg) and temperature (T). Between the atmospheric variables, a basic network between VPD, T, Rg and H remains intact and relatively constant in strength. The dominance of contemporaneous links is found as well, as seen already in Fig. 4. Besides the decoupling of NEE from any variable in the dry period, there are additional interesting patterns. For example, the positive reappearance of the link between NEE and LE in September. Here, the onset of precipitation events (cf. Fig. J1) occurred that lead to strong respiration peaks (Ma et al., 2012). Creating such a network via lagged correlation would result in much more significant links (causing the network to be not interpretable as opposed to PCMCI) and NEE does not decouple from the atmosphere in August (cf. Fig. G1).

The above results demonstrate that PCMCI is sensitive enough to capture seasonal differences and certain physiological reasonable biosphere behaviour. Moreover, PCMCI yields a better interpretable network structure than pure correlation approaches.

### 3.3 ~~Global~~Gridded global data set

Subject of inspection were the significant lags and MCI values of each climatic variable on NDVI. In Fig. 6 the maximal MCI value and the corresponding lag are plotted for the links $X_{t-\tau} \rightarrow \mathrm{NDVI} : \tau \in \{0,1,2,3\}$ with X being one of the climatic drivers radiation, temperature, or precipitation. The chosen significance threshold was set to 0.05. Fig. 7 shows the climatic driver with largest MCI per grid point. PCMCI detects a regionally varying influence of climatic drivers. As expected, the boreal regions are strongly driven by temperature instantaneously, while (semi-) arid regions, which correspond predominantly to grass or prairie dominated areas, respond strongest to precipitation at a time lag of one month. Radiation is found to have a comparatively low spatial effect with hot spots in south and east China, central Russia and east Canada.

The dominant lags are found to be zero and one. Just a very small fraction of the total area shows a maximal MCI value at a higher lag of two or three months. The lags are also not equally distributed among the climatic drivers. Radiation and temperature are predominantly strongest at lag zero, while precipitation has a much larger fraction of area showing the strongest response at lag one. Regions where the impact of Rg on NDVI is strongest at lag 1 tend to respond negatively to Rg but positively to precipitation at lag one. On the other hand, a large part of regions with the strongest impact of precipitation at lag zero respond negatively to it but positively to radiation.

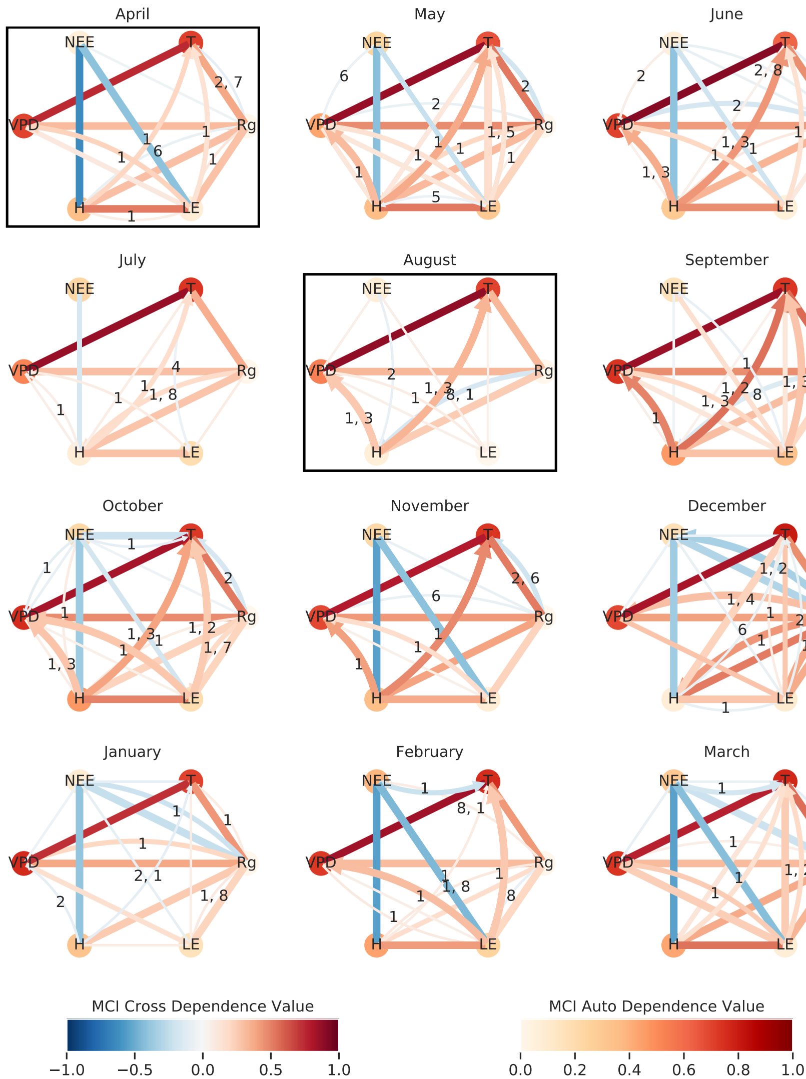


**Figure 5.** To visualize the gradual changes in interaction structure the networks of the three towers are combined for each month. The number of significant occurences of a link is given by its width. The link strength, given by the link color, is calculated by averaging the significant links of the towers. The link's lag is shown in the centre of each arrow, sorted in descending order of link strength. The resulting graphs are shown for April 2014 till March 2015. The significance threshold is 0.01. The networks of April and August, illustrated in Fig. 4, are highlighted by a box.

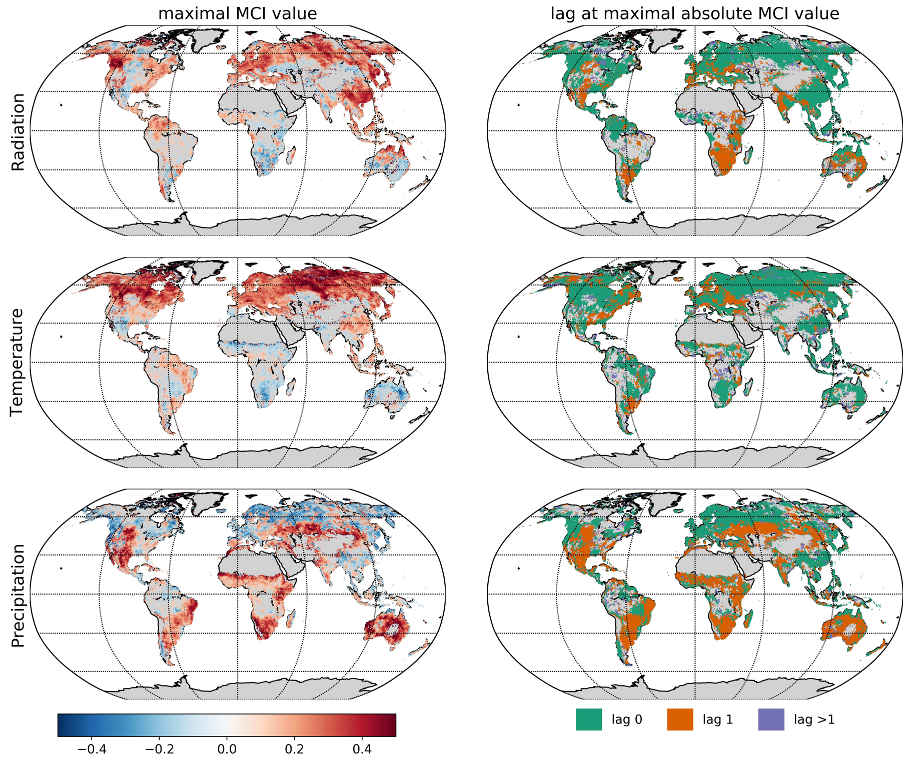


**Figure 6.** Influence of climatic drivers on NDVI as calculated by PCMCI. The first column shows the estimated causal influence given as maximal absolute MCI value of climatic drivers on NDVI. The second column gives the time lag at which the maximal absolute MCI value occures (in month).

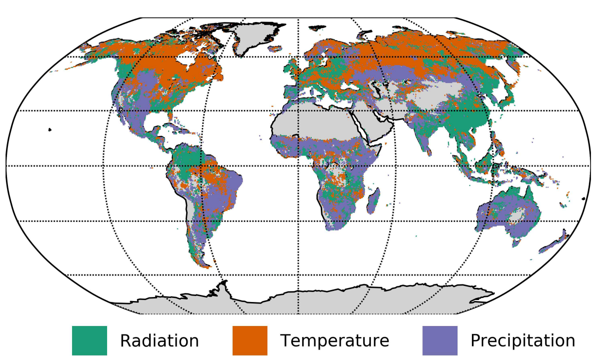


**Figure 7.** Map of the strongest climatic driver (largest absolute MCI value) per grid point.

In summary, PCMCI estimates coherent interaction patterns which match well with anticipated behaviour based on vegetation type and prevailing climatic conditions.

## 4 Discussion

Causal discovery methods promise an improved understanding and can help to come up with new hypotheses about the interaction between biosphere and atmosphere (Christiansen and Peters, 2018; Runge et al., 2019). But the underlying assumptions need to be properly taken into account. The coupled biosphere-atmosphere system possesses several challenges that potentially violate the underlying assumptions of causal discovery in general and the employed method's assumptions in particular. Here, we investigate the effect of a violation of assumptions on PCMCI network estimates.

With regard to expected non-linearities in biosphere-atmosphere interactions, using a linear independence test within the PCMCI framework may not be adequate. We motivate our choice with the following arguments: first, non-linearities are often approximated linearly. Second, a linear regression based test has a much higher power for detecting linear links than a non parametric test (Runge, 2018a) and can, hence, detect links already at smaller sample sizes. Third, linear partial correlation is easily interpretable, for example, positive and negative MCI values. ~~The~~ This motivation is supported on the one hand by the results of the test model ~~support our choices~~and on the other hand by additionally performed analyses on the observational datasets using Gaussian regression and distance correlation as an independence test. These results (cf. Fig. H1,I1,K1) show similar patterns but due to the low sample sizes exhibit lower statistical significances. In general, the derived results show a high detection power with a strong consistency in calculated effect strengths on eddy covariance data and global, regularly gridded reanalysis data that leads to well interpretable patterns. Observed drawbacks are a high FPR in case of violated assumptions, especially strong periodicity, as well as the appearance of contemporaneous lags in measurement datasets.

### 4.1 Lessons learned from the test model

The probability to detect a link with PCMCI depends strongly on a link's MCI effect size, which is larger for strong variance in the driver and a low variance in the receiver ~~(Runge et al., 2018)~~(cf. Sect. 2.5). Several results can be explained by this observation. First, the variance of three out of five drivers of cross dependencies in the test model are either directly or indirectly (via $\mathcal{GPP}$) influenced by $\mathcal{R}g$, which has the highest variance of all variables. Consequently, the detection power of the three links is large, almost 100%. In comparison, the other variables' variances are weaker, since they are influenced by $\mathcal{T}$, which results in a lower detection power. This is the origin of the disparity in detection rates of the non-linear links. Second, also the partially strong increase in TPR of non-linear links (influenced in a multiplicative way by $\mathcal{T}$) from the baseline dataset to the seasonality dataset can be explained by this increase in variance. A multiplicative link is actually not generally expected to be found by ParCorr (Runge, 2018a), but the value of the multiplicative factor is dominated by the seasonal value, and not the dynamical noise, which might cause rather a scaling of the dynamical noise terms rather than a random distortion. Third, the dependence on the variance ratio can also explain the difference in TPR between homoscedastic (equal error variance) and heteroscedastic (error variance changing over time) time series, i.e., the variance of $\mathcal{R}g$ and $\mathcal{GPP}$ exhibits a strong seasonality with its peak in summer, while the variance of $\mathcal{T}$ is rather constant. This explains, for example, the strong decrease in TPR for the link $\mathcal{T} \rightarrow \mathcal{GPP}$ at 91 days time series length when comparing homoscedasticity to heteroscedasticity. The decrease in TPR is less pronounced when another season, implying a different variance, is chosen for this comparison. As links with weak driver variance and strong response variance are more likely to be missed, one may ask which effect this will have on the detection of feedback loops where one variable has low and the other high variance. Here lies a limitation of the test model where no feedback loops were implemented.

Seasonality and heteroscedasticity constitute violations of the stationarity assumption underlying the independence test ParCorr. Seasonality constitutes a common driver in this model. In general, such common drivers increase the dependence among the variables and hence, lead to a higher detection rate for true links (TPR) as well as a higher false positive rate (FPR) for absent links if this driver is not conditioned out properly. This additionally causes the TPR and the FPR rate to increase in the seasonality model. As shown in Runge (2018a), including the cause of the non-stationarity as an exogenous driver in the analysis allows PCMCI to regress out its influence on the other variables. However, for ParCorr this is only valid if the dependence on the non-stationary driver is linear. Therefore, the regression on $\mathcal{R}g$ fails for $\mathcal{GPP}$ and $\mathcal{R}eco$ in the test model. With this ill-posed setting, the probability to detect false links increases with increasing time series length or when more periods are included. Stationarity in mean is obviously also not fully guaranteed when subtracting the seasonal mean. Here we observe that the FPR stays above the significance level for the anomalised seasonality dataset. One can ask whether the FPR stays above the significance threshold because subtracting the seasonal mean does not remove the heteroscedasticity. However, we attribute this high FPR to a not fully removed seasonality since the FPR of both homoscedastic and heteroscedastic time series decreases by roughly the same amount in the anomalised seasonality dataset and the effect of heteroscedasticity is rather weak in the baseline dataset. ~~Much of the influence of heteroscedasticity is also removed when limiting the analysis to a specific time period, i.e. season, which makes the data causally stationarity (cf. Sect. 2.2)~~The increasing FPR with increasing time series length can further raise doubts regarding the analysis of long time series. For such an analysis, though, the assumption of causal stationarity should first be assessed. For example, the link from radiation to GPP vanishes in winter as there is mostly no active plant material left. To account for causal stationarity, the analysis should be limited to time series sections where the causal structure is expected to be similar. This is typically done by limiting the analysis to a specific time period (i.e. 'masking'), e.g. a specific season, month, or time of the day. Such masking reduces additionally further influences of remaining seasonality or heteroscedasticity. One can argue, as it is done in Peters et al. (2017), that the causality of a system is invariant even between seasons ~~,~~ because the physical mechanism is the same in all seasons. Yet, while the physical, i.e. functional relationship might be constant over time, its imprint in the time series might vary. For example, a functional dependence $f(x)$ might be 'flat' for small values of $x$ and linearly increasing for larger values. If only small values occur in the winter season, then the link is absent, while it 'appears' only in the summer season. Across all seasons, this can be considered as a nonlinear functional dependence $f(x)$. In practice, restricting an analysis to different seasons can help in interpreting the mechanism, here in a linear framework.

Summarizing the results of the test model, the different detection rates, disparity among non-linear links, and the detection of multiplicative links are largely explainable via the effect of the variance on the link detection. Yet, the discussion revealed the need for further research in several aspects. On the one hand, feedback loops are not included in the test model yet are an important aspect in natural systems. On the other hand, removing non-stationarities is essential to keep the false positive rate in the expected range, but standard procedures of subtracting the mean seasonal cycle are not sufficient. Further, the effect of non-stationarity on the causal network structure needs to be investigated.

### 4.2 Causal interpretation of estimated networks from observational data

In both the half-hourly time resolved eddy covariance data and the monthly global dataset the predominant type of dependence found is contemporaneous. PCMCI leaves these undirected since no time order indicating the flow of causal information is available. Further, as discussed in Sect. 2.2, contemporaneous common drivers or mediators are not accounted for. The consequence is that both spurious contemporaneous and spurious lagged links can appear, if they are due to contemporaneous variables. For interactions that are contemporaneous in nature since they occur on considerably shorter time scales than the time resolution, therefore, PCMCI is not the optimal choice regarding a causal interpretation and other methods should be applied in conjunction (Runge et al., 2019). Further, we faced a trade off between fulfilling causal assumptions and detection power. In practice, accounting for causal stationarity (by limiting the analysis to certain periods of the dataset) means decreasing the number of available data points while accounting for causal sufficiency leads to an increase in dimensionality by adding variables and increasing the maximal lag. Both will lead to a decrease in detection power, which can affect the network structure. PCMCI alleviates the curse of dimensionality by applying a condition selection step, but still one cannot ~~indefinetly~~ indefinitely add more variables. Another important factor that affects detection power and dimensionality is the time resolution. There are several points in favour and against increasing time resolution. On the one hand, increasing time resolution can resolve contemporaneous links and potentially increases the detection power due to an increased number of datapoints. On the other hand, the dimensionality increases if the maximal lag is adapted. Further, causal information might be split apart and distributed over more lags, rendering the links at each individual lag less detectable. This can cause links to disappear, but links can also appear if new processes are resolved at a higher time scale. At last, observational noise (measurement errors) might be larger in higher resolution data than in aggregated data, as it is averaged out in the latter and thus affects link detection less. Consequently, when comparing network structures based on different settings, i.e. maximal lag, included variables, time resolution, and considered time period, the (dis-)appearance of single links among specific variables can stem from several factors, i.e. a change in detection power, a changed (conditional) dependency, or due to a common driver. These factors together with a non-zero false positive detection rate are challenging for a causal interpretation. Therefore, detected links should be interpreted with care and can give rise to new hypotheses and analyses involving further variables. Generally, a causal interpretation is more robust regarding the absence of links (cf. Sect.2.2). In particular it does not require that all common drivers are observed.

Nevertheless, robust patterns were identified in our studies that are also consistent with other studies. Furthermore, a causal analysis has the advantage of an enhanced interpretability compared to correlative approaches. First of all, we could show that the networks' estimated link strengths are consistent for observational data, even though measurement error affects the data. The dataset used was suitable for this analysis, as the measurement stations are located in a reasonably homogeneous ecosystem that shows only little spatial variation (El-Madany et al., 2018). Thus, also the interaction between biosphere and atmosphere is expected to change only marginally across space within this ecosystem. Second, the gradual changes in plant activity that are taking place in the ecosystem of Majadas throughout the year do very well emerge in the coupling strength of daytime NEE to the atmospheric variables. The observed decoupling during the dry season is in accordance with the one of a soybean field during drought conditions observed by Ruddell and Kumar (2009). The gradual changes in ecosystem activity are not visible in a pure (lagged) correlation analysis or are only visible in color or density changes but the large number of significant links prevents any detailed interpretation on the physical mechanisms and changes thereof. The large number of significant links compared to the PCMCI networks stems solely from the absence of conditioning on common drivers or mediating variables, which often further leads to an overestimation of the link strength in correlation networks. As a result, processes, such as the decoupling of NEE during the dry period, stay hidden. To reduce the effect of confounding, often analyses utilize partial correlation (see e.g. Buermann et al., 2018). However, a partial correlation can introduce new dependencies (as opposed to removing them) if one conditions on causal effects of the variables under consideration (the 'marrying parents' effect). This issue is avoided in PCMCI by only conditioning on past variables. Additionally, PCMCI chooses only relevant variables as conditions by applying the PC condition selection step which is especially valuable in high dimensional study cases and improves detection power and computation time (Runge, 2018a).

The global study of climatic drivers of vegetation shows a general pattern of lags and dependence strengths of vegetation on climatic variables that is easily-interpretable. The boreal regions appear energy limited and especially driven by temperature (cf. Fig 6c), while the strongest dependence of (semi-)arid regions on precipitation reflects their limitation in water supply. Two recent studies performed a similar analysis. Both Wu et al. (2015) and Papagiannopoulou et al. (2017b) investigated lagged effects and dependence strengths of NDVI on precipitation, temperature and radiation. Wu et al. (2015) estimated the lags of the strongest effects via an univariate regression of the climatic drivers on NDVI and subsequently used those lags to fit a multivariate regression model of the climatic drivers on NDVI and determined their relative effects. Papagiannopoulou et al. (2017b) applied a non-linear Granger causality framework utilising a random forest predictive model; the method was presented by Papagiannopoulou et al. (2017a). We recognize that similar patterns are observed in Wu et al. (2015), but the lags at the maximal MCI value are usually lower than the one found in Wu et al. (2015), which stems from the methodical differences. Besides having used anomaly values, PCMCI regresses both NDVI and the climatic drivers on their parents before calculating the MCI value (cf. Sect. 2.5). This especially removes the influence of autocorrelation. Runge et al. (2014) shows how autocorrelation affects the correlative lag causing it to be larger for stronger autocorrelation; thereby the correlative lag may become larger than the causal lag. Therefore, according to Fig. 6b, the causal information embedded in monthly resolution is predominantly received within one month. Finding the strongest causal links at a time lag up to one month appear in agreement with Papagiannopoulou et al. (2017b). Also the spatial distribution of the strongest climatic influences compares well. But there are certain noteworthy differences which not necessarily stem from masking differences, i.e. that we took only values belonging to the growing season while Papagiannopoulou et al. (2017b) took the whole time series. First, there is little significant Granger causality of water availability found in boreal regions while there are significant negative causal dependencies detected via PCMCI. Second, NDVI in arid regions is not or barely Granger caused by radiation and temperature, but in parts shows a negative PCMCI value on those variables. There might be physiological reasons that can explain the PCMCI patterns, i.e. water logging or too high temperatures. To explain the differences though, we could identify two possible reasons. First, Papagiannopoulou et al. (2017b) masked out negative influences of radiation arguing that radiation is not negatively affecting NDVI. They found, that negative influences of Rg are usually a consequence of poor conditioning on other variables. Second, a precipitation event in boreal regions coincides with a reduction in radiation and temperature. Boreal regions usually do not suffer from water shortages. Thus they respond stronger to the reduction of radiation and temperature than precipitation. As precipitation is coupled negatively to radiation and temperature at lag zero, the effect of precipitation on NDVI is found to be negative. Thus, the link P$\overset{-}{\rightarrow}$NDVI might be an effect of the contemporaneous common driver scheme P $\overset{-}{\leftarrow}$ Rg $\overset{+}{\rightarrow}$ NDVI and therefore would not be causal. In fact, a similar argumentation can be given for the negative impact of temperature and radiation on NDVI in arid regions.

In summary, we pointed out the need for careful interpretations in applying causal discovery methods and especially highlighted the challenges linked to the study of biosphere-atmosphere interaction via PCMCI. We demonstrated that the network structures estimated from observational data are explainable with respect to plant physiology and climatic effects. Finally, our study shows that causal methods can deliver better interpretability and a much improved process understanding in comparison to correlation and bivariate Granger causality analyses that are ambiguous to interpret since they do not account for common drivers.

### 4.3 Outlook

The preceding discussion has shed light on the merits of PCMCI as well as the challenges of applying causal discovery methods. Runge et al. (2019) discuss further challenges and methods and give an outlook how multiple methods can be combined to alleviate limitations.

## 5 Conclusions

Here we tested PCMCI, an algorithm that estimates causal graphs from empirical time-series. We specifically explored two types of data sets that are highly relevant in biogeosciences: eddy covariance measurements of land-atmosphere fluxes and global satellite remote sensing of vegetation greenness. The causal graphs estimated from the eddy covariance data collected in a Mediterranean site confirm patterns we would expect in these ecosystems: During the dry season's plants senescence, for instance, the ecosystem's carbon cycle (NEE) decouples from meteorological variability. On the contrary during the main growing season with warm and humid conditions strong links between NEE, LE and H characterise the graph. Not only the strongly contrasting states emerge in the graph structure using the causal framework, but also the gradual transitions that relate to minor changes like the connectivity of sensible heat to temperature with progressing dryness. A purely correlative analysis, instead, is not able to resolve these patterns. PCMCI allows us to identify and focus on much fewer, but highly relevant dependencies only. Applying the approach to three replicated eddy covariance systems shows the robustness of the method to random errors in the fluxes measurements and confirm one of the assumption of eddy covariance: above a relatively homogeneous terrain the fluxes measured should be spatially invariant, and so the underlying causal relationship between climate and fluxes. The global analysis of NDVI in relation to climatic drivers confirms the known patterns of dependence strengths of vegetation on climatic variables: boreal regions are energy limited and especially driven by temperature and secondarily radiation, while in semi-arid regions vegetation dynamics are strongly dependent on water supply. However, obtained response times of vegetation to climatic variations are lower using PCMCI than correlation which can be attributed to a better treatment of the autocorrelation in the time-series and cross-relations among climate variables. Compared to merely correlative approaches, this leads to a interpretable pattern of driver-response relationships. In short, the new developments achieved in causal inference allow to gain well constrained insights on processes, that would otherwise be drowning in the correlation chaos. Therefore we hope that this study fosters usage of causal inference in analysing interactions and feedbacks of the biosphere-atmosphere system and furthermore exhibits our demand of further developments.

**Table A1.** PCMCI parameters that were used differently from default settings.

| Dataset | significance | $\alpha_{pc}$ | tau_min | tau_max | selected_variables | mask_type | fdr_method |
|---|---|---|---|---|---|---|---|
| Test Model | 0.01 | 0.4 | 0 | 25 | [1,2,3] | ’none’ | ’none’ |
| Majadas Dataset | 0.01 | None | 0 | 8 | [1,2,3,4,5] | ’y’ | ’fdr_bh’ |
| Gridded global data set | 0.05 | None | 0 | 3 | [1,2,3] | ’y’ | ’fdr_bh’ |

*Code and data availability.* The eddy covariance data of the FLUXNET sites can be downloaded from the official webpage (https://fluxnet.fluxdata.org/). CRU temperature and precipitation data is available at http://badc.nerc.ac.uk/data/cru/.
CRUNCEP radiation data can be downloaded via ftp://nacp.ornl.gov/synthesis/2009/frescati/temp/land_use_change/original/readme.htm.
The NDVI dataset is available at http://ecocast.arc.nasa.gov/data/pub/gimms/3g/.
The TIGRAMITE software package that includes PCMCI can be found on github https://github.com/jakobrunge/tigramite/. All other code will be made available upon request.

| FLUXNET-ID | start year | end year | Data Reference |
|---|---|---|---|
| AT-Neu | 2002 | 2012 | Wohlfahrt et al. |
| AU-Cpr | 2010 | 2014 | Meyer et al. (2015) |
| AU-DaP | 2007 | 2013 | Beringer et al. (2011a) |
| AU-DaS | 2008 | 2014 | Hutley et al. (2011) |
| AU-Dry | 2008 | 2014 | Cernusak et al. (2011) |
| AU-How | 2001 | 2014 | Beringer et al. (2007) |
| AU-Stp | 2008 | 2014 | Beringer et al. (2011b) |
| AU-Tum | 2001 | 2014 | Leuning et al. (2005) |
| BE-Lon | 2004 | 2014 | Moureaux et al. (2006) |
| BE-Vie | 1996 | 2014 | Aubinet et al. (2001) |
| BR-Sa3 | 2000 | 2004 | Saleska et al. (2003) |
| CA-Man | 1994 | 2008 | Brooks et al. (1997) |
| CA-NS2 | 2001 | 2005 | Bond-Lamberty et al. (2004) |
| CA-NS3 | 2001 | 2005 | Wang et al. (2002a) |
| CA-NS5 | 2001 | 2005 | Wang et al. (2002b) |
| CA-NS6 | 2001 | 2005 | Wang et al. (2002c) |
| CA-Qfo | 2003 | 2010 | Chen et al. (2006) |
| CA-SF2 | 2001 | 2005 | Rayment and Jarvis (1999a) |
| CA-SF3 | 2001 | 2006 | Rayment and Jarvis (1999b) |
| CH-Cha | 2005 | 2014 | Merbold et al. (2014) |
| CH-Dav | 1997 | 2014 | Zielis et al. (2014) |
| CH-Fru | 2005 | 2014 | Imer et al. (2013) |
| CH-Lae | 2004 | 2014 | Etzold et al. (2011) |
| CH-Oe1 | 2002 | 2008 | Ammann et al. (2009) |
| CH-Oe2 | 2004 | 2014 | Dietiker et al. (2010) |
| CZ-wet | 2006 | 2014 | Dušek et al. (2012) |
| DE-Akm | 2009 | 2014 | Bernhofer et al. (a) |
| DE-Geb | 2001 | 2014 | Anthoni et al. (2004) |
| DE-Gri | 2004 | 2014 | Prescher et al. (2010a) |
| DE-Hai | 2000 | 2012 | Knohl et al. (2003a) |
| DE-Kli | 2004 | 2014 | Prescher et al. (2010b) |
| DE-Lkb | 2009 | 2013 | Lindauer et al. (2014) |
| DE-Obe | 2008 | 2014 | Bernhofer et al. (b) |
| DE-Spw | 2010 | 2014 | Bernhofer et al. (c) |
| DE-Tha | 1996 | 2014 | Grünwald and Bernhofer (2007) |
| DK-NuF | 2008 | 2014 | Westergaard-Nielsen et al. (2013) |
| DK-Sor | 1996 | 2014 | Pilegaard et al. (2011) |

| FLUXNET-ID | start year | end year | Data Reference |
|---|---|---|---|
| DK-ZaH | 2000 | 2014 | Lund et al. (2012) |
| FI-Hyy | 1996 | 2014 | Suni et al. (2003) |
| FI-Sod | 2001 | 2014 | Thum et al. (2007) |
| FR-Fon | 2005 | 2014 | Delpierre et al. (2016) |
| FR-LBr | 1996 | 2008 | Berbigier et al. (2001) |
| FR-Pue | 2000 | 2014 | Rambal et al. (2004) |
| GF-Guy | 2004 | 2014 | Bonal et al. (2008) |
| IT-BCi | 2004 | 2014 | Vitale et al. (2016) |
| IT-Col | 1996 | 2014 | Valentini et al. (1996) |
| IT-Lav | 2003 | 2014 | Marcolla et al. (2003) |
| IT-MBo | 2003 | 2013 | Marcolla et al. (2011) |
| IT-Noe | 2004 | 2014 | Spano et al. |
| IT-Ro1 | 2000 | 2008 | Rey et al. (2002) |
| IT-SRo | 1999 | 2012 | Chiesi et al. (2005) |
| IT-Tor | 2008 | 2014 | Galvagno et al. (2013) |
| JP-SMF | 2002 | 2006 | Matsumoto et al. (2008) |
| NL-Hor | 2004 | 2011 | Jacobs et al. (2007) |
| RU-Fyo | 1998 | 2014 | Kurbatova et al. (2008) |
| US-ARM | 2003 | 2012 | Fischer et al. (2007) |
| US-Blo | 1997 | 2007 | Schade et al. |
| US-Ha1 | 1991 | 2012 | Wofsy et al. (1993) |
| US-Me2 | 2002 | 2014 | McDowell et al. (2004) |
| US-Me6 | 2010 | 2014 | Ruehr et al. (2012a) |
| US-MMS | 1999 | 2014 | Pryor et al. (1999) |
| US-Ne1 | 2001 | 2013 | Gitelson et al. (2003) |
| US-Ne2 | 2001 | 2013 | Cassman et al. (2003a) |
| US-Ne3 | 2001 | 2013 | Cassman et al. (2003b) |
| US-SRG | 2008 | 2014 | Ruehr et al. (2012b) |
| US-SRM | 2004 | 2014 | Scott et al. (2008) |
| US-Ton | 2001 | 2014 | Tang et al. (2003) |
| US-Twt | 2009 | 2014 | Hatala et al. (2012) |
| US-UMB | 2000 | 2014 | Rothstein et al. (2000) |
| US-UMd | 2007 | 2014 | Nave et al. (2011) |
| US-Var | 2000 | 2014 | Xu et al. (2004) |
| US-Whs | 2007 | 2014 | Scott et al. (2006) |
| US-Wkg | 2004 | 2014 | Emmerich (2003) |

**Table B1.** List of FLUXNET sites used for the generation of artificial datasets and the time periode used.

**Situation:** A process $\mathbf{X}$ is given.

Process Graph

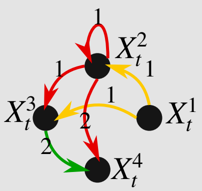

Time series Graph

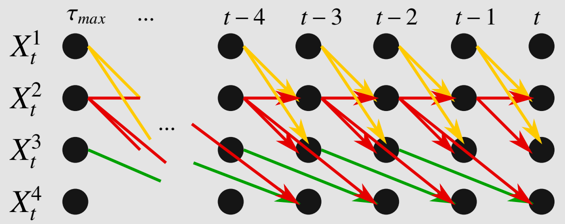

In real world study cases the dependencies of $\mathbf{X}$ are unknown.

**Aim:** To study process $\mathbf{X}$ via graphical models, we need to estimate conditional independence between all variables:

$$X^i_{t-\tau} \not\!\perp\!\!\!\perp X^j_t \mid \mathbf{X}^-_t \setminus \{X^i_{t-\tau}\}$$

**Problem:** Conditioning on the whole past $\mathbf{X}^-_t$ leads to high dimensional estimations.

**PCMCI approach**

1.

**PC-step**

1. Start with a fully connected network

$\widetilde{\mathcal{P}}(X^j_t) = \mathbf{X}^-_t = \{X^i_{t-\tau} : i = 1, ..., N, \tau = 1, ..., \tau_{max}\}$

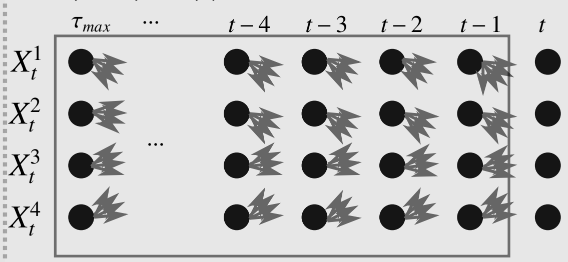

2. Remove nodes from $\widetilde{P}(X^j_t)$ iteratively by keeping nodes that are conditional dependent to $X^j_t$ at a significance level set by the parameter $\alpha_{pc}$ (typically 0.2 - 0.4). Ideally the true parents are still in the set of parents (colored arrows). But likely some spurious parents as well (grey arrows).

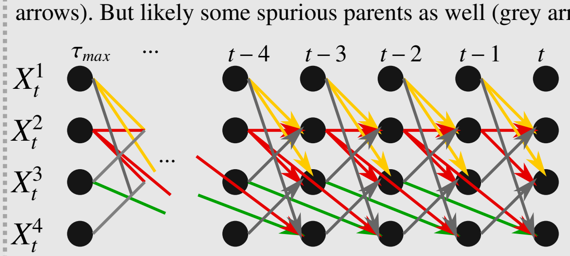

2.

**MCI-step**

1. Perform the conditional independence test for each pair of nodes using their estimated set of parents from the PC-step as conditioning set.

For example a link between $X^2_{t-1}$ und $X^3_t$ exists iff:

$X^2_{t-1} \not\!\perp\!\!\!\perp X^3_t \mid \widetilde{P}(X^2_{t-1}), \widetilde{P}(X^3_t) \setminus \{X^2_{t-1}\}$

with

$\widetilde{P}(X^2_{t-1}) = X^1_{t-2}, X^2_{t-2}, X^3_{t-2}$

$\widetilde{P}(X^3_t) = X^1_{t-1}, X^2_{t-1}, X^4_{t-1}$

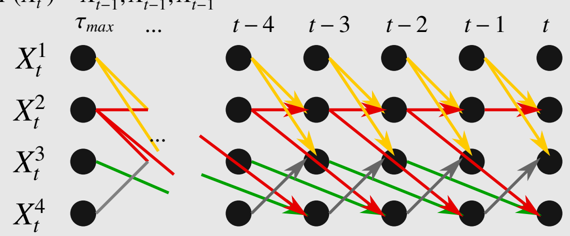

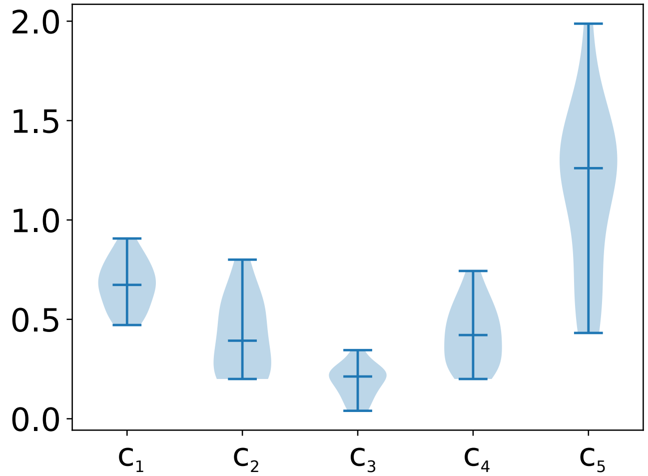


**Figure B1.** Distribution of coupling coefficients obtained after fitting the test model to the Fluxnet sites. Here shown are the distributions used for generation of heteroscedastic time series.

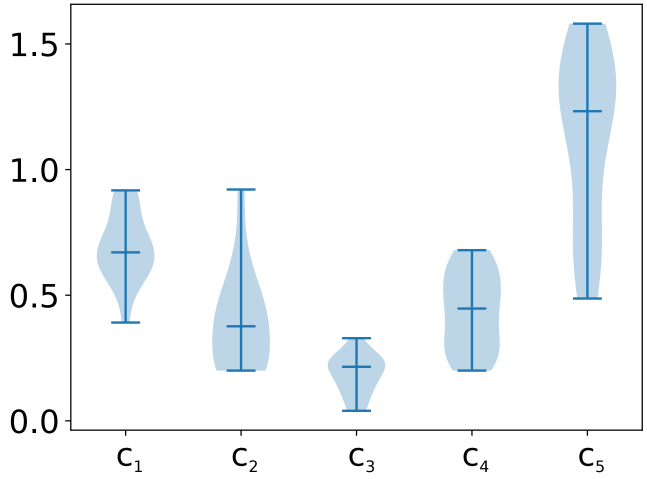


**Figure C1.** Distribution of coupling coefficients obtained after fitting the test model to the Fluxnet sites. Here shown are the distributions used for generation of homoscedastic time series.

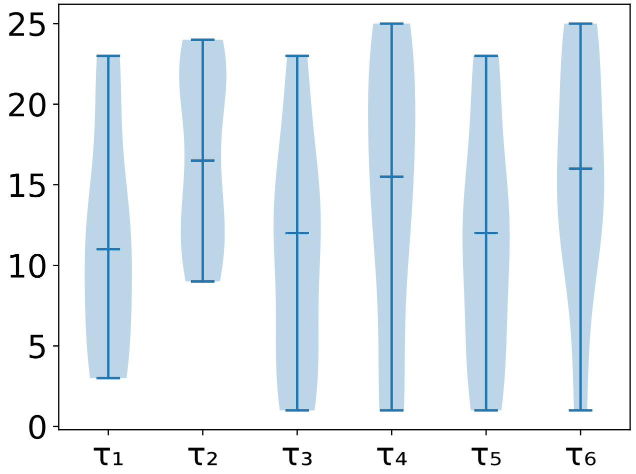


**Figure D1.** Distribution of time lags obtained after fitting the test model to the Fluxnet sites. Here shown are the distributions used for generation of heteroscedastic time series.

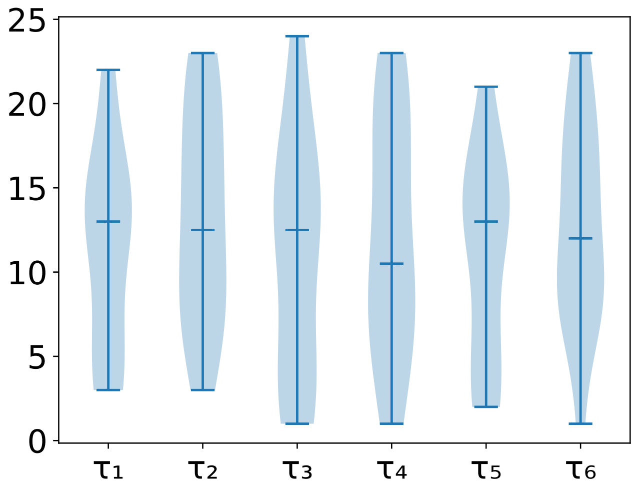


**Figure E1.** Distribution of time lags obtained after fitting the test model to the Fluxnet sites. Here shown are the distributions used for generation of homoscedastic time series.

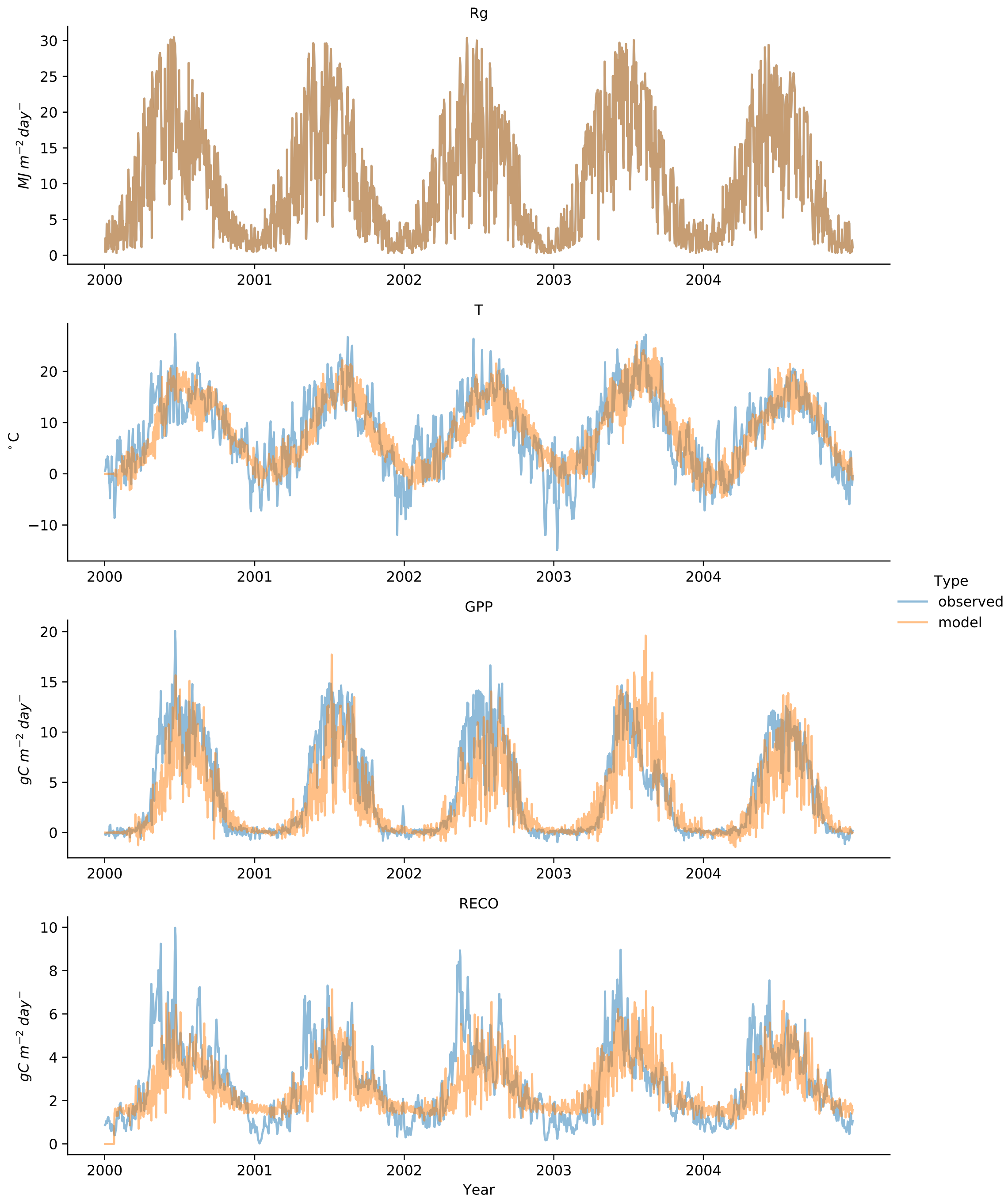


**Figure F1.** Observed (blue) and test model (orange) time-series for Hainich Fluxnet site. The model data was produced with heteroscedastic noise.

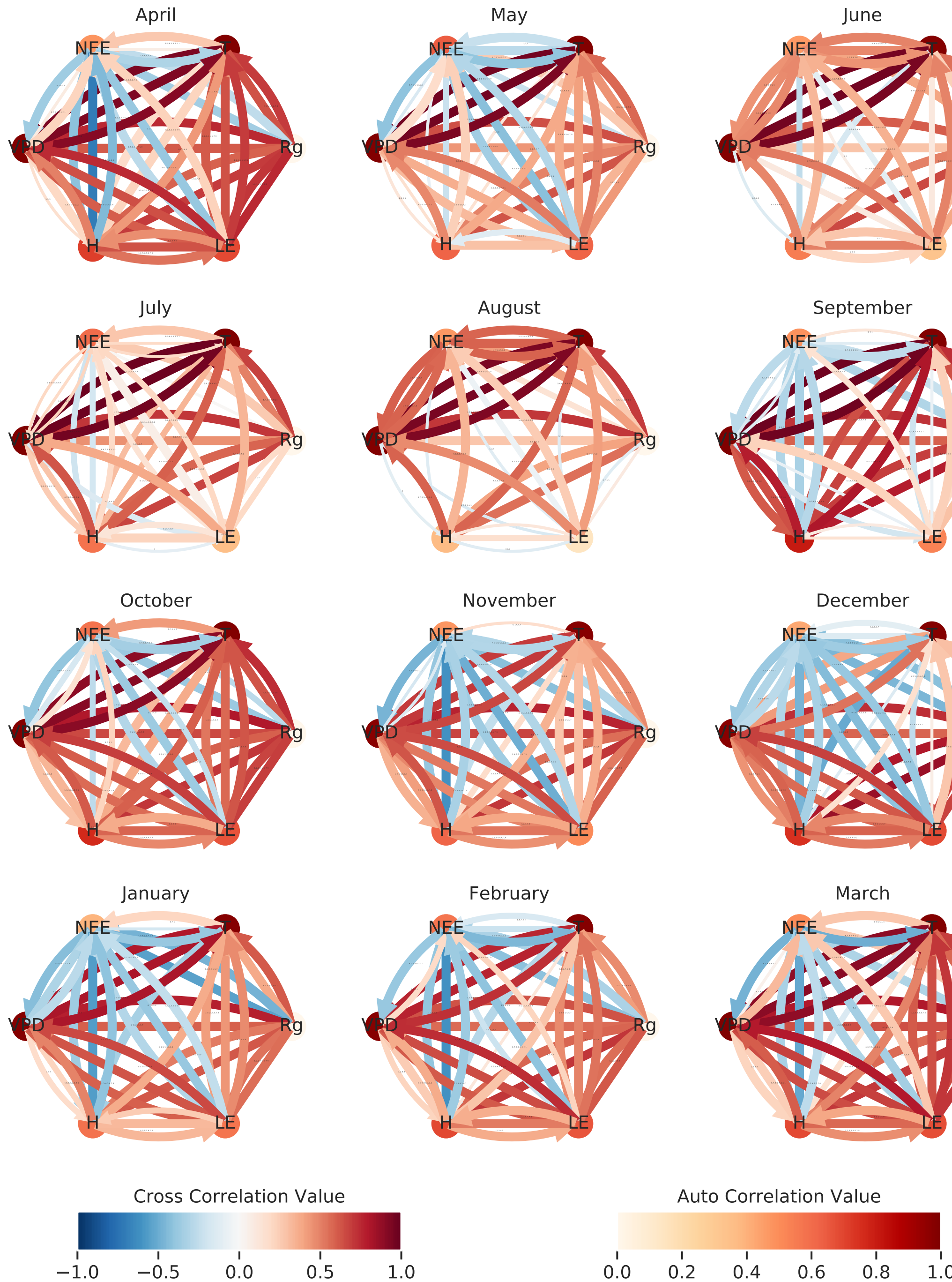


**Figure G1.** Same as Fig. 5 but using simple correlation analysis to estimate the graph structures. The number of significant occurences of a link is given by its width. The link strength, given by the link color, is calculated by averaging the significant links of the towers. Link labels indicating the lag were removed to improve link visibility. They typically ranged from 1 to 8 (full range of possible lags). The resulting graphs are shown for April 2014 till March 2015. The significance threshold is 0.01.

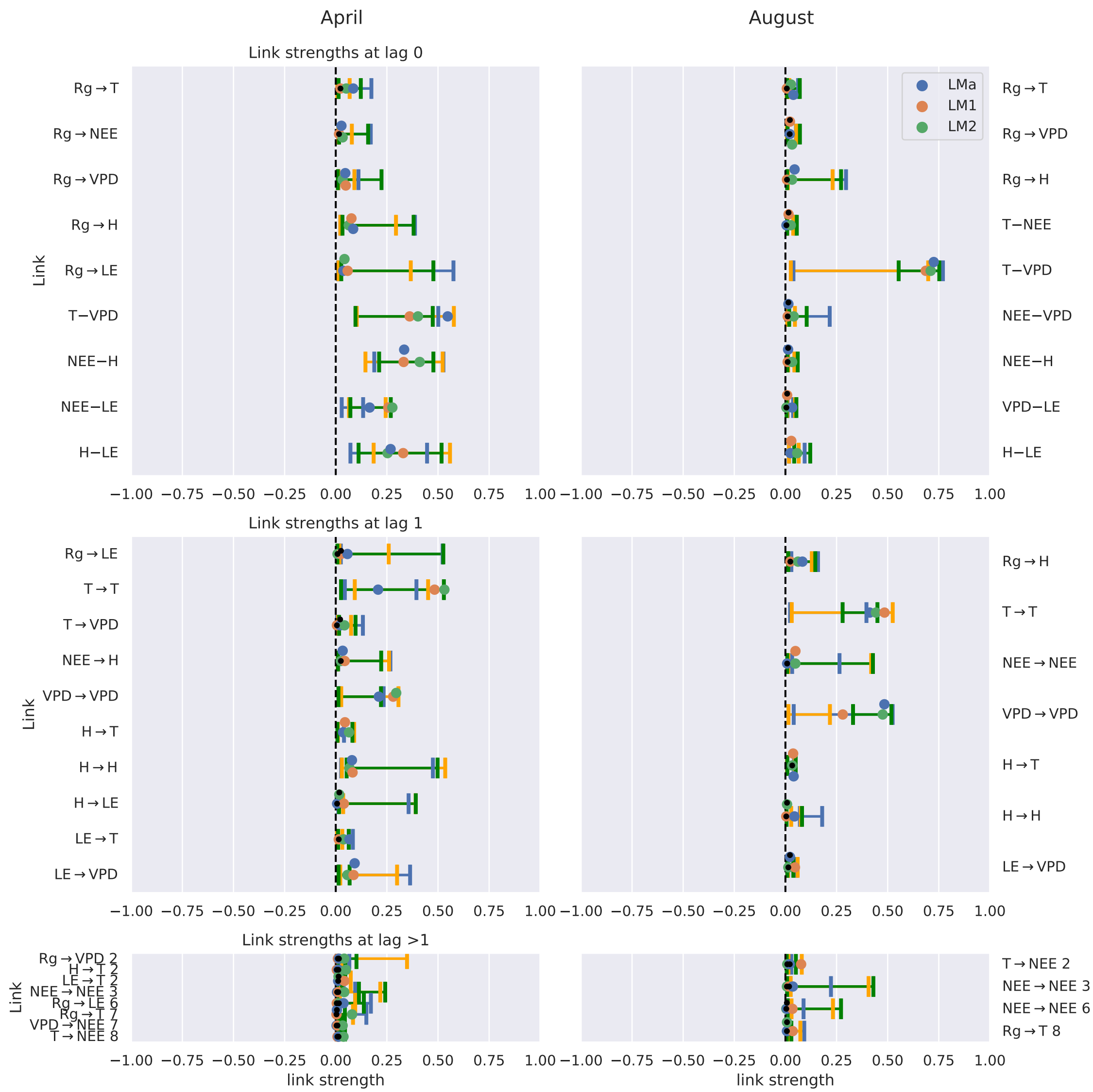


**Figure H1.** Same as Fig. 4 of the manuscript but the analysis was performed using a non-linear independence test. Comparison of the networks of three eddy covariance measurement stations (LMa, LM1, LM2) located in Majadas (Spain). Links that are found to be significant in one of the three networks are included. For each link, the calculated strength of all three networks is plotted with its 90% confidence interval. The colors blue, orange, and green correspond to the towers LMa, LM1, and LM2, respectively. The significance threshold is 0.01. If a link does not pass the significance, it is marked by a black dot. The links are grouped into lag 0 (top), lag 1 (middle) and all lags greater than 1 (bottom). Links at lag 0 are left undirected (−), yet as Rg is set as main driver, links incorporating Rg at lag 0 are directed (→). Note that GPDC only yields positive link strengths. Further, the strength values estimated with GPDC are rather weak due to the low number of datapoints and the larger sensitivity of that method to the sample size

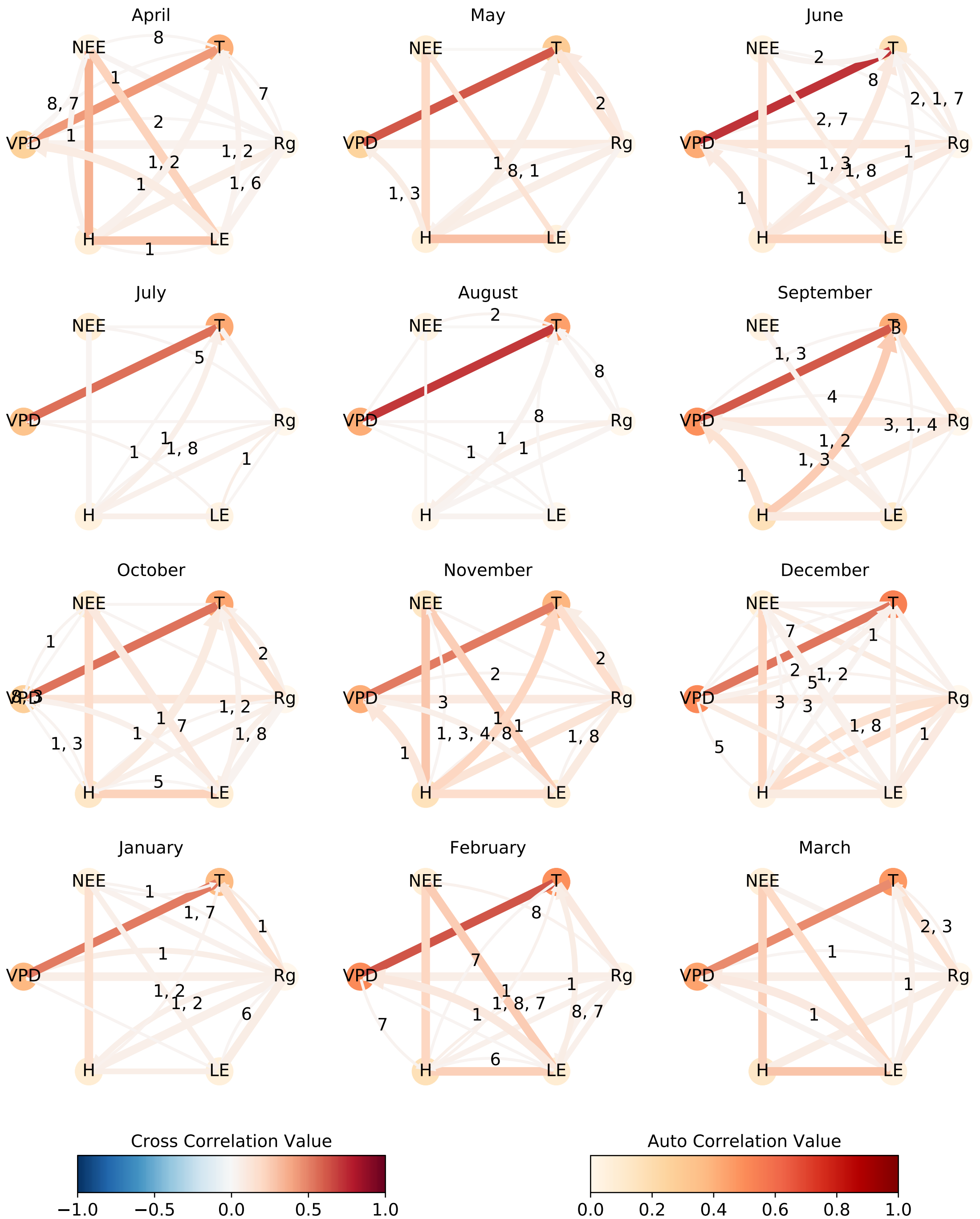


**Figure I1.** Same as Fig. 5 of the manuscript but the analysis was performed using a non-linear independence test. The number of significant occurrences of a link is given by its width. The link strength, given by the link color, is calculated by averaging the significant links of the towers. The link's lag is shown in the centre of each arrow, sorted in descending order of link strength. The resulting graphs are shown for April 2014 till March 2015. The significance threshold is 0.01. Note that GPDC only yields positive link strengths. Further, the strength values estimated with GPDC are rather weak due to the low number of datapoints and the larger sensitivity of that method to the sample size

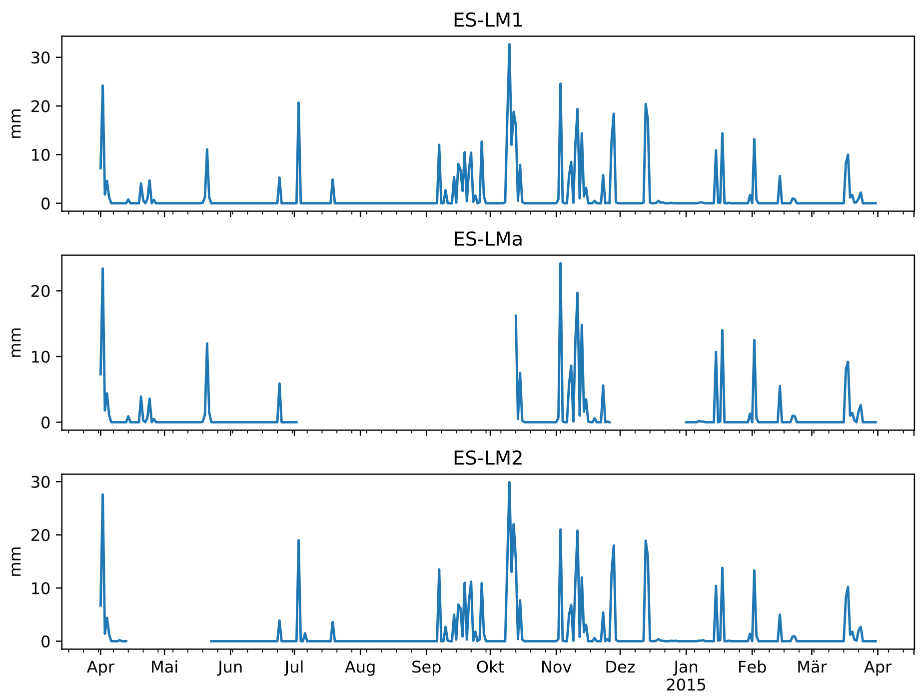


**Figure J1.** ~~Precipitation~~ Daily aggregated precipitation in Majadas ~~Majadas~~ de Tiètar measured at the three tower sites from April 2014 to March 2015. Missing values are ~~set to -1.~~ plotted as gaps.

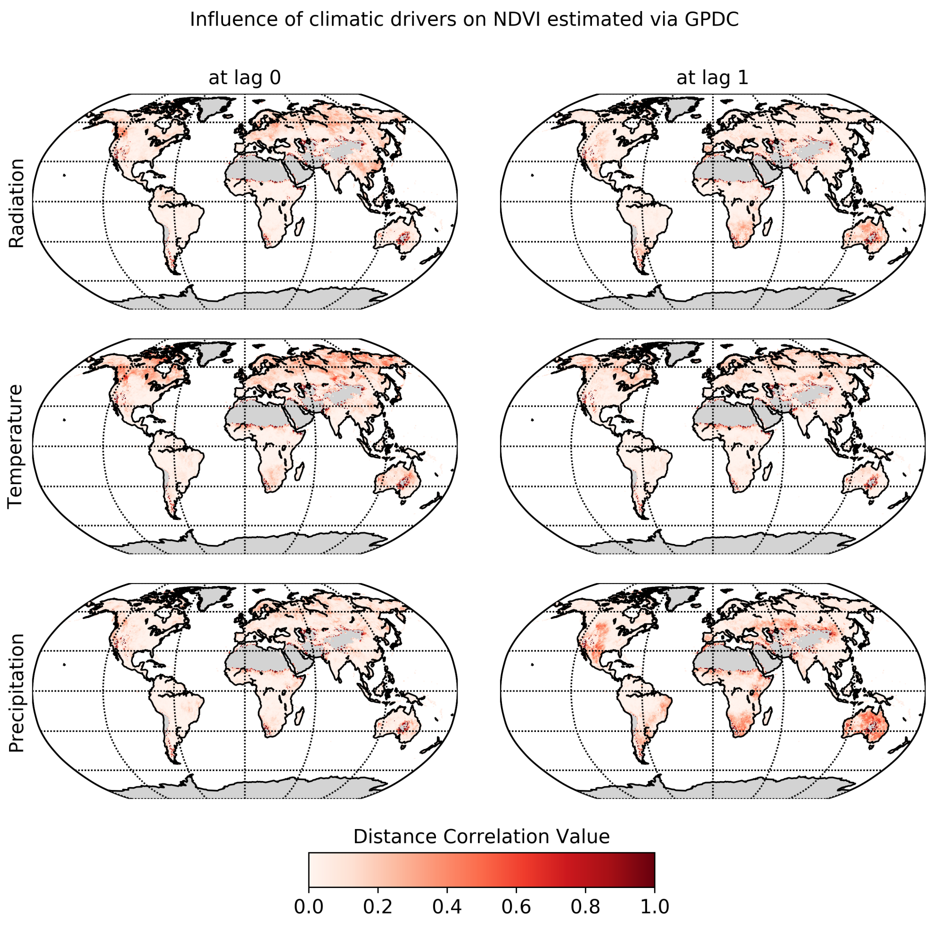


**Figure K1.** Similar to Fig. 3.3 of the manuscript. Influence of climatic drivers on NDVI as calculated by PCMCI in conjunction with the non linear independence test GPDC. The first and second columns show the estimated causal influences of climatic drivers on NDVI at lag 0 and 1, respectively.

*Author contributions.* CK and MDM designed the study with contributions from JR and DGM. CK conducted the analysis and wrote the manuscript. All authors helped to impove the manuscript. AC, MM, TEM, OPP conducted field experiments in Majadas, processed and provided its data as well helped with interpretation.

*Competing interests.* The authors declare that they have no competing interests.

*Acknowledgements.* We thank Maha Shadaydeh, Rune Christiansen, Jonas Peters, Milan Flach and Markus Reichstein for useful comments. CK thanks the Max Planck Research School for global Biogeochemical Cycles for supporting his PhD project. The authors affiliated with 1. thank the European Space Agency for funding the "Earth System Data Lab" project.

This work used eddy covariance data acquired and shared by the FLUXNET community, including these networks: AmeriFlux, AfriFlux, AsiaFlux, CarboAfrica, CarboEuropeIP, CarboItaly, CarboMont, ChinaFlux, Fluxnet-Canada, GreenGrass, ICOS, KoFlux, LBA, NECC, OzFlux-TERN, TCOS-Siberia, and USCCC. The ERA-Interim reanalysis data are provided by ECMWF and processed by LSCE. The FLUXNET eddy covariance data processing and harmonization was carried out by the European Fluxes Database Cluster, AmeriFlux Management Project, and Fluxdata project of FLUXNET, with the support of CDIAC and ICOS Ecosystem Thematic Center, and the OzFlux, ChinaFlux and AsiaFlux offices.

## References


Ammann, C., Spirig, C., Leifeld, J., and Neftel, A.: Assessment of the Nitrogen and Carbon Budget of Two Managed Temperate Grassland Fields, Agriculture, Ecosystems & Environment, 133, 150–162, https://doi.org/10.1016/j.agee.2009.05.006, 2009.

Anthoni, P. M., Knohl, A., Rebmann, C., Freibauer, A., Mund, M., Ziegler, W., Kolle, O., and Schulze, E.-D.: Forest and Agricultural Land-Use-Dependent CO2 Exchange in Thuringia, Germany, Global Change Biology, 10, 2005–2019, https://doi.org/10.1111/j.1365-2486.2004.00863.x, 2004.

Attanasio, A.: Testing for linear Granger causality from natural/anthropogenic forcings to global temperature anomalies, Theoretical and Applied Climatology, 110, 281–289, https://doi.org/10.1007/s00704-012-0634-x, https://doi.org/10.1007/s00704-012-0634-x, 2012.

Attanasio, A., Pasini, A., and Triacca, U.: A contribution to attribution of recent global warming by out-of-sample Granger causality analysis, Atmospheric Science Letters, 13, 67–72, https://doi.org/10.1002/asl.365, https://rmets.onlinelibrary.wiley.com/doi/abs/10.1002/asl.365, 2012.

Aubinet, M., Chermanne, B., Vandenhaute, M., Longdoz, B., Yernaux, M., and Laitat, E.: Long Term Carbon Dioxide Exchange above a Mixed Forest in the Belgian Ardennes, Agricultural and Forest Meteorology, 108, 293–315, https://doi.org/https://doi.org/10.1016/S0168-1923(01)00244-1, 2001.

Baldocchi, D.: Measuring fluxes of trace gases and energy between ecosystems and the atmosphere – the state and future of the eddy covariance method, Global Change Biology, 20, 3600–3609, https://doi.org/10.1111/gcb.12649, http://dx.doi.org/10.1111/gcb.12649, 2014.

Baldocchi, D. D.: Assessing the eddy covariance technique for evaluating carbon dioxide exchange rates of ecosystems: past, present and future, Global Change Biology, 9, 479–492, https://doi.org/10.1046/j.1365-2486.2003.00629.x, https://onlinelibrary.wiley.com/doi/abs/10.1046/j.1365-2486.2003.00629.x, 2003.

Baldocchi, D. D., Hincks, B. B., and Meyers, T. P.: Measuring Biosphere-Atmosphere Exchanges of Biologically Related Gases with Micrometeorological Methods, Ecology, 69, 1331–1340, https://doi.org/10.2307/1941631, https://esajournals.onlinelibrary.wiley.com/doi/abs/10.2307/1941631, 1988.

Baldocchi D, R. Y. and T., K.: Terrestrial Carbon Cycle Variability [version 1; peer review: 2 approved, F1000Research, 5(F1000 Faculty Rev), https://doi.org/(https://doi.org/10.12688/f1000research.8962.1), 2016.

Benjamini, Y. and Hochberg, Y.: Controlling the False Discovery Rate: A Practical and Powerful Approach to Multiple Testing, Journal of the Royal Statistical Society: Series B (Methodological), 57, 289–300, https://doi.org/10.1111/j.2517-6161.1995.tb02031.x, https://rss.onlinelibrary.wiley.com/doi/abs/10.1111/j.2517-6161.1995.tb02031.x, 1995.

Berbigier, P., Bonnefond, J.-M., and Mellmann, P.: CO2 and Water Vapour Fluxes for 2 Years above Euroflux Forest Site, Agricultural and Forest Meteorology, 108, 183–197, https://doi.org/10.1016/S0168-1923(01)00240-4, 2001.

Beringer, J., Hutley, L. B., Tapper, N. J., and Cernusak, L. A.: Savanna Fires and Their Impact on Net Ecosystem Productivity in North Australia, Global Change Biology, 13, {990–1004}, https://doi.org/{10.1111/j.1365-2486.2007.01334.x}, 2007.

Beringer, J., Hutley, L. B., Hacker, J. M., Neininger, B., and U, K. T. P.: Patterns and Processes of Carbon, Water and Energy Cycles across Northern Australian Landscapes: From Point to Region, Agricultural and Forest Meteorology, 151, {1409–1416}, https://doi.org/{10.1016/j.agrformet.2011.05.003}, 2011a.

Beringer, J., Hutley, L. B., Hacker, J. M., Neininger, B., and U, K. T. P.: Patterns and Processes of Carbon, Water and Energy Cycles across Northern Australian Landscapes: From Point to Region, Agricultural and Forest Meteorology, 151, 1409–1416, https://doi.org/https://doi.org/10.1016/j.agrformet.2011.05.003, savanna Patterns of Energy and Carbon Integrated Across the Landscape (SPECIAL), 2011b.

Bernhofer, C., Grünwald, T., Moderow, U., Hehn, M., Eichelmann, U., Prasse, H., and Postel, U.: FLUXNET2015 DE-Akm Anklam, https://doi.org/10.18140/FLX/1440213, a.

Bernhofer, C., Grünwald, T., Moderow, U., Hehn, M., Eichelmann, U., Prasse, H., and Postel, U.: FLUXNET2015 DE-Obe Oberbärenburg, https://doi.org/10.18140/FLX/1440151, b.

Bernhofer, C., Grünwald, T., Moderow, U., Hehn, M., Eichelmann, U., Prasse, H., and Postel, U.: FLUXNET2015 DE-Spw Spreewald, https://doi.org/10.18140/FLX/1440220, c.

Bonal, D., Bosc, A., Ponton, S., Goret, J.-Y., Burban, B., Gross, P., Bonnefond, J.-M., Elbers, J., Longdoz, B., Epron, D., Guehl, J.-M., and Granier, A.: Impact of Severe Dry Season on Net Ecosystem Exchange in the Neotropical Rainforest of French Guiana, Global Change Biology, 14, 1917–1933, https://doi.org/10.1111/j.1365-2486.2008.01610.x, 2008.

Bonan, G.: Ecological Climatology: Concepts and Applications, Cambridge University Press, 3 edn., https://doi.org/10.1017/CBO9781107339200, 2015.

Bond-Lamberty, B., Wang, C., and Gower, S. T.: Net Primary Production and Net Ecosystem Production of a Boreal Black Spruce Wildfire Chronosequence, Global Change Biology, 10, 473–487, https://doi.org/10.1111/j.1529-8817.2003.0742.x, 2004.

Brooks, J. R., Flanagan, L. B., Varney, G. T., and Ehleringer, J. R.: Vertical gradients in photosynthetic gas exchange characteristics and refixation of respired CO2 within boreal forest canopies, Tree Physiology, 17, 1–12, https://doi.org/10.1093/treephys/17.1.1, https://doi.org/10.1093/treephys/17.1.1, 1997.

Buermann, W., Forkel, M., O'Sullivan, M., Sitch, S., Friedlingstein, P., Haverd, V., K. Jain, A., Kato, E., Kautz, M., Lienert, S., Lombardozzi, D., E. M. S. Nabel, J., Tian, H., J. Wiltshire, A., Zhu, D., Smith, W., and D. Richardson, A.: Widespread seasonal compensation effects of spring warming on northern plant productivity, Nature, 562, https://doi.org/10.1038/s41586-018-0555-7, 2018.

Cassman, K. G., Dobermann, A., Walters, D. T., and Yang, H.: Meeting Cereal Demand While Protecting Natural Resources and Improving Environmental Quality, Annual Review of Environment and Resources, 28, 315–358, https://doi.org/10.1146/annurev.energy.28.040202.122858, 2003a.

Cassman, K. G., Dobermann, A., Walters, D. T., and Yang, H.: Meeting Cereal Demand While Protecting Natural Resources and Improving Environmental Quality, Annual Review of Environment and Resources, 28, 315–358, https://doi.org/10.1146/annurev.energy.28.040202.122858, 2003b.

Cernusak, L. A., Hutley, L. B., Beringer, J., Holtum, J. A. M., and Turner, B. L.: Photosynthetic Physiology of Eucalypts along a Sub-Continental Rainfall Gradient in Northern Australia, Agricultural and Forest Meteorology, 151, {1462–1470}, https://doi.org/{10.1016/j.agrformet.2011.01.006}, 2011.

Chen, J. M., Govind, A., Sonnentag, O., Zhang, Y., Barr, A., and Amiro, B.: Leaf Area Index Measurements at Fluxnet-Canada Forest Sites, Agricultural and Forest Meteorology, 140, 257–268, https://doi.org/10.1016/j.agrformet.2006.08.005, 2006.

Chiesi, M., Maselli, F., Bindi, M., Fibbi, L., Cherubini, P., Arlotta, E., Tirone, G., Matteucci, G., and Seufert, G.: Modelling Carbon Budget of Mediterranean Forests Using Ground and Remote Sensing Measurements, Agricultural and Forest Meteorology, 135, 22–34, https://doi.org/10.1016/j.agrformet.2005.09.011, 2005.

Christiansen, R. and Peters, J.: Switching Regression Models and Causal Inference in the Presence of Latent Variables, arXiv preprint arXiv:1808.05541, 2018.

Delpierre, N., Berveiller, D., Granda, E., and Dufrêne, E.: Wood Phenology, Not Carbon Input, Controls the Interannual Variability of Wood Growth in a Temperate Oak Forest, New Phytologist, 210, 459–470, https://doi.org/10.1111/nph.13771, 2016.

Detto, M., Molini, A., Katul, G., Stoy, P., Palmroth, S., and Baldocchi, D.: Causality and Persistence in Ecological Systems: A Nonparametric Spectral Granger Causality Approach., The American Naturalist, 179, 524–535, https://doi.org/10.1086/664628, https://doi.org/10.1086/664628, pMID: 22437181, 2012.

Dietiker, D., Buchmann, N., and Eugster, W.: Testing the Ability of the DNDC Model to Predict CO2 and Water Vapour Fluxes of a Swiss Cropland Site, Agriculture, Ecosystems & Environment, 139, 396–401, https://doi.org/10.1016/j.agee.2010.09.002, 2010.

Dušek, J., Čížková, H., Stellner, S., Czerný, R., and Květ, J.: Fluctuating Water Table Affects Gross Ecosystem Production and Gross Radiation Use Efficiency in a Sedge-Grass Marsh, Hydrobiologia, 692, 57–66, https://doi.org/10.1007/s10750-012-0998-z, 2012.

Ebert-Uphoff, I. and Deng, Y.: Causal Discovery for Climate Research Using Graphical Models, Journal of Climate, 25, 5648–5665, https://doi.org/10.1175/JCLI-D-11-00387.1, https://doi.org/10.1175/JCLI-D-11-00387.1, 2012.

El-Madany, T. S., Reichstein, M., Perez-Priego, O., Carrara, A., Moreno, G., Martín, M. P., Pacheco-Labrador, J., Wohlfahrt, G., Nieto, H., Weber, U., Kolle, O., Luo, Y.-P., Carvalhais, N., and Migliavacca, M.: Drivers of spatio-temporal variability of carbon dioxide and energy fluxes in a Mediterranean savanna ecosystem, Agricultural and Forest Meteorology, 262, 258 – 278, https://doi.org/https://doi.org/10.1016/j.agrformet.2018.07.010, http://www.sciencedirect.com/science/article/pii/S0168192318302314, 2018.

Elsner, J. B.: Evidence in support of the climate change–Atlantic hurricane hypothesis, Geophysical Research Letters, 33, https://doi.org/10.1029/2006GL026869, https://agupubs.onlinelibrary.wiley.com/doi/abs/10.1029/2006GL026869, 2006.

Elsner, J. B.: Granger causality and Atlantic hurricanes, Tellus A: Dynamic Meteorology and Oceanography, 59, 476–485, https://doi.org/10.1111/j.1600-0870.2007.00244.x, https://doi.org/10.1111/j.1600-0870.2007.00244.x, 2007.

Emmerich, W. E.: Carbon Dioxide Fluxes in a Semiarid Environment with High Carbonate Soils, Agricultural and Forest Meteorology, 116, 91–102, https://doi.org/10.1016/S0168-1923(02)00231-9, 2003.

Etzold, S., Ruehr, N. K., Zweifel, R., Dobbertin, M., Zingg, A., Pluess, P., Häsler, R., Eugster, W., and Buchmann, N.: The Carbon Balance of Two Contrasting Mountain Forest Ecosystems in Switzerland: Similar Annual Trends, but Seasonal Differences, Ecosystems, 14, 1289–1309, https://doi.org/10.1007/s10021-011-9481-3, 2011.

Fischer, M. L., Billesbach, D. P., Berry, J. A., Riley, W. J., and Torn, M. S.: Spatiotemporal Variations in Growing Season Exchanges of CO2, H2O, and Sensible Heat in Agricultural Fields of the Southern Great Plains, Earth Interactions, 11, 1–21, https://doi.org/10.1175/EI231.1, 2007.

Galvagno, M., Wohlfahrt, G., Cremonese, E., Rossini, M., Colombo, R., Filippa, G., Julitta, T., Manca, G., Siniscalco, C., di Cella, U. M., and Migliavacca, M.: Phenology and Carbon Dioxide Source/Sink Strength of a Subalpine Grassland in Response to an Exceptionally Short Snow Season, Environmental Research Letters, 8, 025 008, https://doi.org/10.1088/1748-9326/8/2/025008, 2013.

Gerken, T., Ruddell, B. L., Fuentes, J. D., Araújo, A., Brunsell, N. A., Maia, J., Manzi, A., Mercer, J., dos Santos, R. N., von Randow, C., and Stoy, P. C.: Investigating the mechanisms responsible for the lack of surface energy balance closure in a central Amazonian tropical rainforest, Agricultural and Forest Meteorology, 255, 92 – 103, https://doi.org/https://doi.org/10.1016/j.agrformet.2017.03.023, http://www.sciencedirect.com/science/article/pii/S0168192317301260, honoring W.J. Massman's Discoveries: Bringing Physics to Agriculture, 2018.

Gitelson, A. A., Viña, A., Arkebauer, T. J., Rundquist, D. C., Keydan, G., and Leavitt, B.: Remote Estimation of Leaf Area Index and Green Leaf Biomass in Maize Canopies, Geophysical Research Letters, 30, https://doi.org/10.1029/2002GL016450, 2003.

Goodwell, A. E. and Kumar, P.: Temporal Information Partitioning Networks (TIPNets): A process network approach to infer ecohydrologic shifts, Water Resources Research, 53, 5899–5919, https://doi.org/10.1002/2016WR020218, https://agupubs.onlinelibrary.wiley.com/doi/abs/10.1002/2016WR020218, 2017a.

Goodwell, A. E. and Kumar, P.: Temporal information partitioning: Characterizing synergy, uniqueness, and redundancy in interacting environmental variables, Water Resources Research, 53, 5920–5942, https://doi.org/10.1002/2016WR020216, https://agupubs.onlinelibrary.wiley.com/doi/abs/10.1002/2016WR020216, 2017b.

Goodwell, A. E., Kumar, P., Fellows, A. W., and Flerchinger, G. N.: Dynamic process connectivity explains ecohydrologic responses to rainfall pulses and drought, Proceedings of the National Academy of Sciences, 115, E8604–E8613, https://doi.org/10.1073/pnas.1800236115, https://www.pnas.org/content/115/37/E8604, 2018.

Granger, C. W. J.: Investigating Causal Relations by Econometric Models and Cross-spectral Methods, Econometrica, 37, 424–438, http://www.jstor.org/stable/1912791, 1969.

Green, J., G. Konings, A., Alemohammad, S. H., Berry, J., Entekhabi, D., Kolassa, J., Lee, J.-E., and Gentine, P.: Regionally strong feedbacks between the atmosphere and terrestrial biosphere, NATURE GEOSCIENCE, 10, 410–414, https://doi.org/http://dx.doi.org/10.1038/ngeo2957, https://www.nature.com/ngeo/journal/v10/n6/pdf/ngeo2957.pdf, 2017.

Grünwald, T. and Bernhofer, C.: A Decade of Carbon, Water and Energy Flux Measurements of an Old Spruce Forest at the Anchor Station Tharandt, Tellus B: Chemical and Physical Meteorology, 59, 387–396, https://doi.org/10.1111/j.1600-0889.2007.00259.x, 2007.

Guanter, L., Kaufmann, H., Segl, K., Foerster, S., Rogass, C., Chabrillat, S., Kuester, T., Hollstein, A., Rossner, G., Chlebek, C., Straif, C., Fischer, S., Schrader, S., Storch, T., Heiden, U., Mueller, A., Bachmann, M., Mühle, H., Müller, R., Habermeyer, M., Ohndorf, A., Hill, J., Buddenbaum, H., Hostert, P., Van der Linden, S., Leitão, P. J., Rabe, A., Doerffer, R., Krasemann, H., Xi, H., Mauser, W., Hank, T., Locherer, M., Rast, M., Staenz, K., and Sang, B.: The EnMAP Spaceborne Imaging Spectroscopy Mission for Earth Observation, Remote Sensing, 7, 8830–8857, https://doi.org/10.3390/rs70708830, https://www.mdpi.com/2072-4292/7/7/8830, 2015.

Harris, I., Jones, P., Osborn, T., and Lister, D.: Updated high-resolution grids of monthly climatic observations – the CRU TS3.10 Dataset, International Journal of Climatology, 34, 623–642, https://doi.org/10.1002/joc.3711, https://rmets.onlinelibrary.wiley.com/doi/abs/10.1002/joc.3711, 2014.

Hatala, J. A., Detto, M., and Baldocchi, D. D.: Gross Ecosystem Photosynthesis Causes a Diurnal Pattern in Methane Emission from Rice, Geophysical Research Letters, 39, https://doi.org/10.1029/2012GL051303, 2012.

Hlaváčková-Schindler, K., Paluš, M., Vejmelka, M., and Bhattacharya, J.: Causality detection based on information-theoretic approaches in time series analysis, Physics Reports, 441, 1 – 46, https://doi.org/https://doi.org/10.1016/j.physrep.2006.12.004, http://www.sciencedirect.com/science/article/pii/S0370157307000403, 2007.

Hutley, L. B., Beringer, J., Isaac, P. R., Hacker, J. M., and Cernusak, L. A.: A Sub-Continental Scale Living Laboratory: Spatial Patterns of Savanna Vegetation over a Rainfall Gradient in Northern Australia, Agricultural and Forest Meteorology, 151, {1417–1428}, https://doi.org/{10.1016/j.agrformet.2011.03.002}, 2011.

Imer, D., Merbold, L., Eugster, W., and Buchmann, N.: Temporal and Spatial Variations of Soil $CO_2$, $CH_4$ and $N_2O$ Fluxes at Three Differently Managed Grasslands, Biogeosciences, 10, 5931–5945, https://doi.org/https://doi.org/10.5194/bg-10-5931-2013, 2013.

Jacobs, C. M. J., Jacobs, A. F. G., Bosveld, F. C., Hendriks, D. M. D., Hensen, A., Kroon, P. S., Moors, E. J., Nol, L., Schrier-Uijl, A., and Veenendaal, E. M.: Variability of Annual $CO_2$ Exchange from Dutch Grasslands, Biogeosciences, 4, 803–816, https://doi.org/https://doi.org/10.5194/bg-4-803-2007, 2007.

James, R. G., Barnett, N., and Crutchfield, J. P.: Information Flows? A Critique of Transfer Entropies, Phys. Rev. Lett., 116, 238 701, https://doi.org/10.1103/PhysRevLett.116.238701, https://link.aps.org/doi/10.1103/PhysRevLett.116.238701, 2016.

Justice, C., Townshend, J., Vermote, E., Masuoka, E., Wolfe, R., Saleous, N., Roy, D., and Morisette, J.: An overview of MODIS Land data processing and product status, Remote Sensing of Environment, 83, 3 – 15, https://doi.org/https://doi.org/10.1016/S0034-4257(02)00084-6, http://www.sciencedirect.com/science/article/pii/S0034425702000846, the Moderate Resolution Imaging Spectroradiometer (MODIS): a new generation of Land Surface Monitoring, 2002.

Knohl, A., Schulze, E.-D., Kolle, O., and Buchmann, N.: Large Carbon Uptake by an Unmanaged 250-Year-Old Deciduous Forest in Central Germany, Agricultural and Forest Meteorology, 118, 151–167, https://doi.org/10.1016/S0168-1923(03)00115-1, 2003a.

Knohl, A., Schulze, E.-D., Kolle, O., and Buchmann, N.: Large carbon uptake by an unmanaged 250-year-old deciduous forest in Central Germany, Agricultural and Forest Meteorology, 118, 151 – 167, https://doi.org/https://doi.org/10.1016/S0168-1923(03)00115-1, http://www.sciencedirect.com/science/article/pii/S0168192303001151, 2003b.

Kodra, E., Chatterjee, S., and Ganguly, A. R.: Exploring Granger causality between global average observed time series of carbon dioxide and temperature, Theoretical and Applied Climatology, 104, 325–335, https://doi.org/10.1007/s00704-010-0342-3, https://doi.org/10.1007/s00704-010-0342-3, 2011.

Kretschmer, M., Coumou, D., Donges, J. F., and Runge, J.: Using Causal Effect Networks to Analyze Different Arctic Drivers of Midlatitude Winter Circulation, Journal of Climate, 29, 4069–4081, https://doi.org/10.1175/JCLI-D-15-0654.1, https://doi.org/10.1175/JCLI-D-15-0654.1, 2016.

Kumar, P. and Ruddell, B.: Information driven ecohydrologic self-organization, Entropy, 12, 2085–2096, https://doi.org/10.3390/e12102085, 2010.

Kurbatova, J., Li, C., Varlagin, A., Xiao, X., and Vygodskaya, N.: Modeling Carbon Dynamics in Two Adjacent Spruce Forests with Different Soil Conditions in Russia, Biogeosciences, 5, 969–980, https://doi.org/https://doi.org/10.5194/bg-5-969-2008, 2008.

Leuning, R., Cleugh, H. A., Zegelin, S. J., and Hughes, D.: Carbon and Water Fluxes over a Temperate Eucalyptus Forest and a Tropical Wet/Dry Savanna in Australia: Measurements and Comparison with MODIS Remote Sensing Estimates, Agricultural and Forest Meteorology, 129, 151–173, https://doi.org/https://doi.org/10.1016/j.agrformet.2004.12.004, 2005.

Lindauer, M., Schmid, H. P., Grote, R., Mauder, M., Steinbrecher, R., and Wolpert, B.: Net Ecosystem Exchange over a Non-Cleared Wind-Throw-Disturbed Upland Spruce Forest—Measurements and Simulations, Agricultural and Forest Meteorology, 197, 219–234, https://doi.org/10.1016/j.agrformet.2014.07.005, 2014.

Lund, M., Falk, J. M., Friborg, T., Mbufong, H. N., Sigsgaard, C., Soegaard, H., and Tamstorf, M. P.: Trends in CO2 Exchange in a High Arctic Tundra Heath, 2000–2010, Journal of Geophysical Research: Biogeosciences, 117, https://doi.org/10.1029/2011JG001901, 2012.

Ma, S., Baldocchi, D. D., Hatala, J. A., Detto, M., and Yuste, J. C.: Are rain-induced ecosystem respiration pulses enhanced by legacies of antecedent photodegradation in semi-arid environments?, Agricultural and Forest Meteorology, 154-155, 203 – 213, https://doi.org/https://doi.org/10.1016/j.agrformet.2011.11.007, http://www.sciencedirect.com/science/article/pii/S0168192311003364, 2012.

Malenovský, Z., Rott, H., Cihlar, J., Schaepman, M. E., García-Santos, G., Fernandes, R., and Berger, M.: Sentinels for science: Potential of Sentinel-1, -2, and -3 missions for scientific observations of ocean, cryosphere, and land, Remote Sensing of Environment, 120, 91 – 101, https://doi.org/https://doi.org/10.1016/j.rse.2011.09.026, http://www.sciencedirect.com/science/article/pii/S0034425712000648, the Sentinel Missions - New Opportunities for Science, 2012.

Marcolla, B., Pitacco, A., and Cescatti, A.: Canopy Architecture and Turbulence Structure in a Coniferous Forest, Boundary-Layer Meteorology, 108, 39–59, https://doi.org/10.1023/A:1023027709805, 2003.

Marcolla, B., Cescatti, A., Manca, G., Zorer, R., Cavagna, M., Fiora, A., Gianelle, D., Rodeghiero, M., Sottocornola, M., and Zampedri, R.: Climatic Controls and Ecosystem Responses Drive the Inter-Annual Variability of the Net Ecosystem Exchange of an Alpine Meadow, Agricultural and Forest Meteorology, 151, 1233–1243, https://doi.org/10.1016/j.agrformet.2011.04.015, 2011.

Matsumoto, K., Ohta, T., Nakai, T., Kuwada, T., Daikoku, K., Iida, S., Yabuki, H., Kononov, A. V., van der Molen, M. K., Kodama, Y., Maximov, T. C., Dolman, A. J., and Hattori, S.: Energy Consumption and Evapotranspiration at Several Boreal and Temperate Forests in the Far East, Agricultural and Forest Meteorology, 148, 1978–1989, https://doi.org/10.1016/j.agrformet.2008.09.008, 2008.

McDowell, N. G., Bowling, D. R., Bond, B. J., Irvine, J., Law, B. E., Anthoni, P., and Ehleringer, J. R.: Response of the Carbon Isotopic Content of Ecosystem, Leaf, and Soil Respiration to Meteorological and Physiological Driving Factors in a Pinus Ponderosa Ecosystem, Global Biogeochemical Cycles, 18, https://doi.org/10.1029/2003GB002049, 2004.

McPherson, R. A.: A review of vegetation—atmosphere interactions and their influences on mesoscale phenomena, Progress in Physical Geography, 31, 261–285, https://doi.org/10.1177/0309133307079055, https://doi.org/10.1177/0309133307079055, 2007.

Merbold, L., Eugster, W., Stieger, J., Zahniser, M., Nelson, D., and Buchmann, N.: Greenhouse Gas Budget (CO2, CH4 and N2O) of Intensively Managed Grassland Following Restoration, Global Change Biology, 20, 1913–1928, https://doi.org/10.1111/gcb.12518, 2014.

Meyer, W. S., Kondrlova, E., and Koerber, G. R.: Evaporation of Perennial Semi-Arid Woodland in Southeastern Australia Is Adapted for Irregular but Common Dry Periods, Hydrological Processes, 29, {3714–3726}, https://doi.org/{10.1002/hyp.10467}, 2015.

Miralles, D. G., Gentine, P., Seneviratne, S. I., and Teuling, A. J.: Land–atmospheric feedbacks during droughts and heatwaves: state of the science and current challenges, Annals of the New York Academy of Sciences, 0, https://doi.org/10.1111/nyas.13912, https://nyaspubs.onlinelibrary.wiley.com/doi/abs/10.1111/nyas.13912, 2018.

Mogensen, P. K. and Riseth, A. N.: Optim: A mathematical optimization package for Julia, Journal of Open Source Software, 3, 615, https://doi.org/10.21105/joss.00615, 2018.

Monson, R. and Baldocchi, D.: Terrestrial Biosphere-Atmosphere Fluxes, Cambridge University Press, https://doi.org/10.1017/CBO9781139629218, 2014.

Moureaux, C., Debacq, A., Bodson, B., Heinesch, B., and Aubinet, M.: Annual Net Ecosystem Carbon Exchange by a Sugar Beet Crop, Agricultural and Forest Meteorology, 139, 25–39, https://doi.org/https://doi.org/10.1016/j.agrformet.2006.05.009, 2006.

Nave, L. E., Gough, C. M., Maurer, K. D., Bohrer, G., Hardiman, B. S., Moine, J. L., Munoz, A. B., Nadelhoffer, K. J., Sparks, J. P., Strahm, B. D., Vogel, C. S., and Curtis, P. S.: Disturbance and the Resilience of Coupled Carbon and Nitrogen Cycling in a North Temperate Forest, Journal of Geophysical Research: Biogeosciences, 116, https://doi.org/10.1029/2011JG001758, 2011.

Papagiannopoulou, C., Miralles, D. G., Decubber, S., Demuzere, M., Verhoest, N. E. C., Dorigo, W. A., and Waegeman, W.: A non-linear Granger-causality framework to investigate climate–vegetation dynamics, Geoscientific Model Development, 10, 1945–1960, https://doi.org/10.5194/gmd-10-1945-2017, https://www.geosci-model-dev.net/10/1945/2017/, 2017a.

Papagiannopoulou, C., Miralles, D. G., Dorigo, W. A., Verhoest, N. E. C., Depoorter, M., and Waegeman, W.: Vegetation anomalies caused by antecedent precipitation in most of the world, Environmental Research Letters, 12, 074 016, http://stacks.iop.org/1748-9326/12/i=7/a=074016, 2017b.

Pearl, J.: Causality, Cambridge University Press, https://doi.org/10.1017/CBO9780511803161, 2009.

Peters, J., Janzing, D., and Schölkopf, B.: Elements of Causal Inference: Foundations and Learning Algorithms, MIT Press, Cambridge, MA, USA, 2017.

Pilegaard, K., Ibrom, A., Courtney, M. S., Hummelshøj, P., and Jensen, N. O.: Increasing Net CO2 Uptake by a Danish Beech Forest during the Period from 1996 to 2009, Agricultural and Forest Meteorology, 151, 934–946, https://doi.org/10.1016/j.agrformet.2011.02.013, 2011.

Pinzon, J. E. and Tucker, C. J.: A Non-Stationary 1981–2012 AVHRR NDVI3g Time Series, Remote Sensing, 6, 6929–6960, https://doi.org/10.3390/rs6086929, http://www.mdpi.com/2072-4292/6/8/6929, 2014.

Prescher, A.-K., Grünwald, T., and Bernhofer, C.: Land Use Regulates Carbon Budgets in Eastern Germany: From NEE to NBP, Agricultural and Forest Meteorology, 150, 1016–1025, https://doi.org/10.1016/j.agrformet.2010.03.008, 2010a.

Prescher, A.-K., Grünwald, T., and Bernhofer, C.: Land Use Regulates Carbon Budgets in Eastern Germany: From NEE to NBP, Agricultural and Forest Meteorology, 150, 1016–1025, https://doi.org/10.1016/j.agrformet.2010.03.008, 2010b.

Pryor, S. C., Barthelmie, R. J., and Jensen, B.: Nitrogen Dry Deposition at an AmeriFlux Site in a Hardwood Forest in the Midwest, Geophysical Research Letters, 26, 691–694, https://doi.org/10.1029/1999GL900066, 1999.

Qi, W. and Dubayah, R. O.: Combining Tandem-X InSAR and simulated GEDI lidar observations for forest structure mapping, Remote Sensing of Environment, 187, 253 – 266, https://doi.org/https://doi.org/10.1016/j.rse.2016.10.018, http://www.sciencedirect.com/science/article/pii/S003442571630390X, 2016.

Rambal, S., Joffre, R., Ourcival, J. M., Cavender-Bares, J., and Rocheteau, A.: The Growth Respiration Component in Eddy CO2 Flux from a Quercus Ilex Mediterranean Forest, Global Change Biology, 10, 1460–1469, https://doi.org/10.1111/j.1365-2486.2004.00819.x, 2004.

Rayment, M. B. and Jarvis, P. G.: Seasonal Gas Exchange of Black Spruce Using an Automatic Branch Bag System, Canadian Journal of Forest Research, 29, 1528–1538, https://doi.org/10.1139/x99-130, 1999a.

Rayment, M. B. and Jarvis, P. G.: Seasonal Gas Exchange of Black Spruce Using an Automatic Branch Bag System, Canadian Journal of Forest Research, 29, 1528–1538, https://doi.org/10.1139/x99-130, 1999b.

Rey, A., Pegoraro, E., Tedeschi, V., Parri, I. D., Jarvis, P. G., and Valentini, R.: Annual Variation in Soil Respiration and Its Components in a Coppice Oak Forest in Central Italy, Global Change Biology, 8, 851–866, https://doi.org/10.1046/j.1365-2486.2002.00521.x, 2002.

Rothstein, D. E., Zak, D. R., Pregitzer, K. S., and Curtis, P. S.: Kinetics of Nitrogen Uptake by Populus Tremuloides in Relation to Atmospheric CO2 and Soil Nitrogen Availability, Tree Physiology, 20, 265–270, https://doi.org/10.1093/treephys/20.4.265, 2000.

Ruddell, B., Yu, R., Kang, M., and Childers, D.: Seasonally varied controls of climate and phenophase on terrestrial carbon dynamics: modeling eco-climate system state using Dynamical Process Networks, Landscape Ecology, https://doi.org/10.1007/s10980-015-0253-x, 2015.

Ruddell, B. L. and Kumar, P.: Ecohydrologic process networks: 1. Identification, Water Resources Research, 45, n/a–n/a, https://doi.org/10.1029/2008WR007279, http://dx.doi.org/10.1029/2008WR007279, w03419, 2009.

Ruehr, N. K., Martin, J. G., and Law, B. E.: Effects of Water Availability on Carbon and Water Exchange in a Young Ponderosa Pine Forest: Above- and Belowground Responses, Agricultural and Forest Meteorology, 164, 136–148, https://doi.org/10.1016/j.agrformet.2012.05.015, 2012a.

Ruehr, N. K., Martin, J. G., and Law, B. E.: Effects of Water Availability on Carbon and Water Exchange in a Young Ponderosa Pine Forest: Above- and Belowground Responses, Agricultural and Forest Meteorology, 164, 136–148, https://doi.org/10.1016/j.agrformet.2012.05.015, 2012b.

Runge, J.: Causal network reconstruction from time series: From theoretical assumptions to practical estimation, Chaos: An Interdisciplinary Journal of Nonlinear Science, 28, 075 310, https://doi.org/10.1063/1.5025050, https://doi.org/10.1063/1.5025050, 2018a.

Runge, J.: TIGRAMITE-Causal discovery for time series datasets, https://github.com/jakobrunge/tigramite/, 2018b.

Runge, J., Heitzig, J., Marwan, N., and Kurths, J.: Quantifying causal coupling strength: A lag-specific measure for multivariate time series related to transfer entropy, Phys. Rev. E, 86, 061 121, https://doi.org/10.1103/PhysRevE.86.061121, https://link.aps.org/doi/10.1103/PhysRevE.86.061121, 2012a.

Runge, J., Heitzig, J., Petoukhov, V., and Kurths, J.: Escaping the Curse of Dimensionality in Estimating Multivariate Transfer Entropy, Phys. Rev. Lett., 108, 258 701, https://doi.org/10.1103/PhysRevLett.108.258701, https://link.aps.org/doi/10.1103/PhysRevLett.108.258701, 2012b.

Runge, J., Petoukhov, V., and Kurths, J.: Quantifying the Strength and Delay of Climatic Interactions: The Ambiguities of Cross Correlation and a Novel Measure Based on Graphical Models, Journal of Climate, 27, 720–739, https://doi.org/10.1175/JCLI-D-13-00159.1, https://doi.org/10.1175/JCLI-D-13-00159.1, 2014.

Runge, J., Nowack, P., Kretschmer, M., Flaxman, S., and Sejdinovic, D.: Detecting causal associations in large nonlinear time series datasets, arXiv e-prints, arXiv:1702.07007v2, https://arxiv.org/abs/1702.07007v2, 2018.

Runge, J., Bathiany, S., Bollt, E., Camps-Valls, G., Coumou, D., Deyle, E., Glymour, C., Kretschmer, M., Mahecha, M. D., Muñoz-Marí, J., et al.: Inferring causation from time series in Earth system sciences, Nature communications, 10, 2553, 2019.

Saleska, S. R., Miller, S. D., Matross, D. M., Goulden, M. L., Wofsy, S. C., da Rocha, H. R., de Camargo, P. B., Crill, P., Daube, B. C., de Freitas, H. C., Hutyra, L., Keller, M., Kirchhoff, V., Menton, M., Munger, J. W., Pyle, E. H., Rice, A. H., and Silva, H.: Carbon in Amazon Forests: Unexpected Seasonal Fluxes and Disturbance-Induced Losses, Science, 302, 1554–1557, https://doi.org/10.1126/science.1091165, 2003.

Schade, G. W., Goldstein, A. H., and Lamanna, M. S.: Are Monoterpene Emissions Influenced by Humidity?, Geophysical Research Letters, 26, 2187–2190, https://doi.org/10.1029/1999GL900444.

Schreiber, T.: Measuring Information Transfer, Phys. Rev. Lett., 85, 461–464, https://doi.org/10.1103/PhysRevLett.85.461, https://link.aps.org/doi/10.1103/PhysRevLett.85.461, 2000.

Scott, R. L., Huxman, T. E., Cable, W. L., and Emmerich, W. E.: Partitioning of Evapotranspiration and Its Relation to Carbon Dioxide Exchange in a Chihuahuan Desert Shrubland, Hydrological Processes, 20, 3227–3243, https://doi.org/10.1002/hyp.6329, 2006.

Scott, R. L., Cable, W. L., and Hultine, K. R.: The Ecohydrologic Significance of Hydraulic Redistribution in a Semiarid Savanna, Water Resources Research, 44, https://doi.org/10.1029/2007WR006149, 2008.

Shadaydeh, M., Garcia, Y. G., Mahecha, M., Reichstein, M., and Denzler, J.: Analyzing the Time Variant Causality in Ecological Time Series: A Time-Frequency Approach, in: International Conference on Ecological Informatics (ICEI), pp. 151–152, 2018.

Shannon, C.: A Mathematical Theory of Communication, Bell System Technical Journal, 27, 379–423, https://doi.org/10.1002/j.1538-7305.1948.tb01338.x, https://www2.scopus.com/inward/record.uri?eid=2-s2.0-84940644968&doi=10.1002%2fj.1538-7305.1948.tb01338.x&partnerID=40&md5=8164c9f2519a48647f6ea2d501b98177, cited By 13847, 1948.

Smirnov, D. A.: Spurious causalities with transfer entropy, Phys. Rev. E, 87, 042 917, https://doi.org/10.1103/PhysRevE.87.042917, https://link.aps.org/doi/10.1103/PhysRevE.87.042917, 2013.

Spano, D., Duce, P., Marras, S., Sirca, C., Arca, A., Zara, P., Ventura, A., Mereu, S., and Sanna, L.: FLUXNET2015 IT-Noe Arca di Noe - Le Prigionette, https://doi.org/10.18140/FLX/1440171.

Spirtes, P. and Glymour, C.: An Algorithm for Fast Recovery of Sparse Causal Graphs, Social Science Computer Review, 9, 62–72, https://doi.org/10.1177/089443939100900106, https://doi.org/10.1177/089443939100900106, 1991.

Spirtes, P., Glymour, C., and Scheines, R.: Causation, prediction, and search, MIT Press, 2001.

Suni, T., Rinne, J., Reissell, A., Altimir, N., Keronen, P., Rannik, U., Dal Maso, M., Kulmala, M., and Vesala, T.: Long-Term Measurements of Surface Fluxes above a Scots Pine Forest in Hyytiala, Southern Finland, 1996-2001, BOREAL ENVIRONMENT RESEARCH, 8, {287–301}, 2003.

Tang, J., Baldocchi, D. D., Qi, Y., and Xu, L.: Assessing Soil CO2 Efflux Using Continuous Measurements of CO2 Profiles in Soils with Small Solid-State Sensors, Agricultural and Forest Meteorology, 118, 207–220, https://doi.org/10.1016/S0168-1923(03)00112-6, 2003.

Thum, T., Aalto, T., Laurila, T., Aurela, M., Kolari, P., and Hari, P.: Parametrization of Two Photosynthesis Models at the Canopy Scale in a Northern Boreal Scots Pine Forest, Tellus B, 59, 874–890, https://doi.org/10.1111/j.1600-0889.2007.00305.x, 2007.

Valentini, R., Angelis, P. D., Matteucci, G., Monaco, R., Dore, S., and Mucnozza, G. E. S.: Seasonal Net Carbon Dioxide Exchange of a Beech Forest with the Atmosphere, Global Change Biology, 2, 199–207, https://doi.org/10.1111/j.1365-2486.1996.tb00072.x, 1996.

Viovy, N.: CRUNCEP data set, availableat:ftp://nacp.ornl.gov/synthesis/2009/frescati/temp/land_use_change/original/readme.htm, lastaccess:June2016, 2016.

Vitale, L., Di Tommasi, P., D'Urso, G., and Magliulo, V.: The Response of Ecosystem Carbon Fluxes to LAI and Environmental Drivers in a Maize Crop Grown in Two Contrasting Seasons, International Journal of Biometeorology, 60, 411–420, https://doi.org/10.1007/s00484-015-1038-2, 2016.

Wang, C., Bond-Lamberty, B., and Gower, S. T.: Environmental Controls on Carbon Dioxide Flux from Black Spruce Coarse Woody Debris, Oecologia, 132, 374–381, https://doi.org/10.1007/s00442-002-0987-4, 2002a.

Wang, C., Bond-Lamberty, B., and Gower, S. T.: Environmental Controls on Carbon Dioxide Flux from Black Spruce Coarse Woody Debris, Oecologia, 132, 374–381, https://doi.org/10.1007/s00442-002-0987-4, 2002b.

Wang, C., Bond-Lamberty, B., and Gower, S. T.: Environmental Controls on Carbon Dioxide Flux from Black Spruce Coarse Woody Debris, Oecologia, 132, 374–381, https://doi.org/10.1007/s00442-002-0987-4, 2002c.

Westergaard-Nielsen, A., Lund, M., Hansen, B. U., and Tamstorf, M. P.: Camera Derived Vegetation Greenness Index as Proxy for Gross Primary Production in a Low Arctic Wetland Area, ISPRS Journal of Photogrammetry and Remote Sensing, 86, 89–99, https://doi.org/10.1016/j.isprsjprs.2013.09.006, 2013.

Wofsy, S. C., Goulden, M. L., Munger, J. W., Fan, S.-M., Bakwin, P. S., Daube, B. C., Bassow, S. L., and Bazzaz, F. A.: Net Exchange of CO2 in a Mid-Latitude Forest, Science, 260, 1314–1317, https://doi.org/10.1126/science.260.5112.1314, 1993.

Wohlfahrt, G., Hammerle, A., Haslwanter, A., Bahn, M., Tappeiner, U., and Cernusca, A.: Seasonal and inter-annual variability of the net ecosystem CO2 exchange of a temperate mountain grassland: Effects of weather and management, Journal of Geophysical Research: Atmospheres, 113, https://doi.org/10.1029/2007JD009286, https://agupubs.onlinelibrary.wiley.com/doi/abs/10.1029/2007JD009286.

Woodcock, C. E., Allen, R., Anderson, M., Belward, A., Bindschadler, R., Cohen, W., Gao, F., Goward, S. N., Helder, D., Helmer, E., Nemani, R., Oreopoulos, L., Schott, J., Thenkabail, P. S., Vermote, E. F., Vogelmann, J., Wulder, M. A., and Wynne, R.: Free Access to Landsat Imagery, Science, 320, 1011–1011, https://doi.org/10.1126/science.320.5879.1011a, https://science.sciencemag.org/content/320/5879/1011.1, 2008.

Wright, S.: Correlation and causation, J. Agric. Res., 20, 557–580, https://ci.nii.ac.jp/naid/10010273333/en/, 1921.

Wu, D., Zhao, X., Liang, S., Zhou, T., Huang, K., Tang, B., and Zhao, W.: Time-lag effects of global vegetation responses to climate change, Global Change Biology, 21, 3520–3531, https://doi.org/10.1111/gcb.12945, https://onlinelibrary.wiley.com/doi/abs/10.1111/gcb.12945, 2015.

Xu, L., Baldocchi, D. D., and Tang, J.: How Soil Moisture, Rain Pulses, and Growth Alter the Response of Ecosystem Respiration to Temperature, Global Biogeochemical Cycles, 18, https://doi.org/10.1029/2004GB002281, 2004.

Yu, R., Ruddell, B. L., Kang, M., Kim, J., and Childers, D.: Anticipating global terrestrial ecosystem state change using FLUXNET, Global Change Biology, 25, 2352–2367, https://doi.org/10.1111/gcb.14602, https://onlinelibrary.wiley.com/doi/abs/10.1111/gcb.14602, 2019.

Zielis, S., Etzold, S., Zweifel, R., Eugster, W., Haeni, M., and Buchmann, N.: NEP of a Swiss Subalpine Forest Is Significantly Driven Not Only by Current but Also by Previous Year's Weather, Biogeosciences, 11, 1627–1635, https://doi.org/https://doi.org/10.5194/bg-11-1627-2014, 2014.